

# Unraveling the Role of Ctla-4 in Intestinal Immune Homeostasis: Insights from a novel Zebrafish Model of Inflammatory Bowel Disease

Lulu Qin, Chongbin Hu, Qiong Zhao, Yong Wang, Dongdong Fan, Aifu Lin, Lixin Xiang , Ye Chen , Jianzhong Shao 

College of Life Sciences, Key Laboratory for Cell and Gene Engineering of Zhejiang Province, Zhejiang University, Hangzhou, China • Department of Genetic and Metabolic Disease, the Children's Hospital, Zhejiang University School of Medicine, National Clinical Research Center for Child Health, Hangzhou 310052, China • Laboratory for Marine Biology and Biotechnology, Qingdao National Laboratory for Marine Science and Technology, Qingdao, China

 [https://en.wikipedia.org/wiki/Open\\_access](https://en.wikipedia.org/wiki/Open_access)

 Copyright information

## Abstract

Inflammatory bowel disease (IBD) is a chronic and relapsing immune-mediated disorder characterized by intestinal inflammation and epithelial injury. The underlying causes of IBD are not fully understood, but genetic factors have implicated in genome-wide association studies, including CTLA-4, an essential negative regulator of T cell activation. However, establishing a direct link between CTLA-4 and IBD has been challenging due to the early lethality of CTLA-4 knockout mice. In this study, we identified zebrafish Ctla-4 homolog and investigated its role in maintaining intestinal immune homeostasis by generating a Ctla-4-deficient (*ctla-4<sup>-/-</sup>*) zebrafish line. These mutant zebrafish exhibit reduced weight, along with impaired epithelial barrier integrity and lymphocytic infiltration in their intestines. Transcriptomics analysis revealed upregulation of inflammation-related genes, disturbing immune system homeostasis. Moreover, single-cell RNA-sequencing analysis indicated increased Th2 cells and interleukin 13 expression, along with decreased innate lymphoid cells and upregulated proinflammatory cytokines. Additionally, Ctla-4-deficient zebrafish exhibited reduced diversity and an altered composition of the intestinal microbiota. All these phenotypes closely resemble those found in mammalian IBD. Lastly, supplementation with Ctla-4-Ig successfully alleviated intestinal inflammation in these mutants. Altogether, our findings demonstrate the pivotal role of Ctla-4 in maintaining intestinal homeostasis. Additionally, they offer substantial evidence linking CTLA-4 to IBD and establish a novel zebrafish model for investigating both the pathogenesis and potential treatments.

### eLife assessment

This study focuses on the role of a T-cell-specific receptor, *ctla-4*, in a new zebrafish model of IBD-like phenotype. Although implicated in IBD diseases, the function of *ctla-4* has been hard to study in mice as the KO is lethal. *Ctla-4* mutant zebrafish exhibited significant intestinal inflammation and dysbiosis, mirroring the pathology of inflammatory bowel disease (IBD) in mammals, providing a new **valuable** model to the field of IBD research. However, although many of the results are **solid**, the methods as provided are **incomplete**, without information on methods for many data panels.

<https://doi.org/10.7554/eLife.101932.1.sa3>

## Introduction

Inflammatory bowel disease (IBD), including Crohn's disease and ulcerative colitis, refers to a group of chronic relapsing inflammation disorders affecting the gastrointestinal tract, that have been increasing in prevalence worldwide [1]. The precise etiology of IBD has yet to be fully elucidated. Conventional epidemiological studies have indicated that IBD tends to run in families and is linked to genetic factors [2, 3]. However, research also suggested that susceptibility gene patterns differ significantly among various geographic populations. Current evidence points towards a complicated interaction involving host genetics, disrupted intestinal microbiota, environmental triggers, and abnormal immune responses [4–6]. Advances in genomic sequencing techniques have allowed for the identification of genetic variants associated with an increased risk of developing IBD. Among these, mutations in immune-related genes have received particular attention. Research on humans with Crohn's disease and mouse models of IBD has shown that genetically susceptible individuals exhibit defects in intracellular pattern-recognition receptors (PRRS), such as toll-like receptors (TLR) and nucleotide-binding oligomerization domain (NOD)-like receptors (NLRs), which are responsible for initiating innate immune responses to eliminate harmful bacteria [7, 8]. Genetic variations in the tumor necrosis factor ligand superfamily member 15 (TNFSF15) and interleukin 23 receptor (IL23R) genes, both involved in suppressing inflammation, have been associated with an increased risk of developing Crohn's disease [9, 10].

Cytotoxic T-cell associated antigen-4 (CTLA-4), also known as CD152, is one of the most well-established immune checkpoint molecules expressed predominantly on T cells. It primarily regulates the early stages of T-cell activation by attenuating downstream signaling of the T cell receptor (TCR) [11–13]. Specifically, CTLA-4 has a much higher affinity for CD80 and CD86 ligands compared to the co-stimulatory receptor CD28 [14, 15]. By outcompeting CD28 for ligand binding, CTLA-4 provides an inhibitory signal that impacts immunological synapse formation and inhibits T-cell proliferation and activation [13, 16]. As expected, links between polymorphic alleles of CTLA4 and IBD have been reported in multiple studies [17–19]. Moreover, CTLA-4 is an intriguing target for novel immune checkpoint blockade therapies in cancer treatment, while intestinal inflammation is a common side effect in these clinical trials [20, 21]. Establishing a direct causal relationship between CTLA-4 and IBD has been challenging due to difficulties in finding appropriate models. Early lethality was observed in CTLA-4-deficient mice, adding to the complexity of this issue. Zebrafish is a powerful model system for immunological and biomedical research, due to its versatility and high degree of conservation in innate and adaptive immunities. In our current study, we identified the *Ctla-4* homology in zebrafish and successfully developed an adult vertebrate model with homozygous knockout of the

*ctla-4* gene for the first time. These *ctla-4*-deficient (*ctla-4*<sup>-/-</sup>) zebrafish survive but exhibit attenuated growth and weight loss. Notably, *ctla-4* deficiency leads to an IBD-like phenotype in zebrafish characterized by altered intestinal epithelial cells morphology, abnormal inflammatory response, defects in microbial stratification and composition. Mechanistically, Ctla-4 exerts its inhibitory function by competing with Cd28 for binding to Cd80/86. These findings establish the *ctla-4* knockout zebrafish as an innovative platform to elucidate CTLA-4 immunobiology, model human IBD, and develop novel therapeutic modalities.

## Results

### Identification of zebrafish Ctla-4

Through a homology search in the NCBI database, we identified the *ctla-4* gene on zebrafish chromosome 9 (Fig. S1A–C). Zebrafish Ctla-4 protein contains an N-terminal signal peptide, a single IgV-like extracellular domain, a transmembrane region, and a cytoplasmic tail (Fig. 1A). A <sup>113</sup>LFPPPY<sup>118</sup> motif is present in the ectodomain of Ctla-4, similar to the MYPPPY motif, a binding site for CD80/CD86 found in mammals (Fig. 1A). Thus, we reasoned that the <sup>113</sup>LFPPPY<sup>118</sup> motif may be a potential binding site for Cd80/86 in zebrafish. The tyrosine-based YVKM motif in the cytoplasmic domain in mammals, which is involved in internalization and signaling inhibition, is absent in Ctla-4. By contrast, a unique tyrosine-based <sup>206</sup>YVKF<sup>209</sup> motif was found in the C-terminus of Ctla-4 molecule, which is relatively conserved in different fish species (Fig. 1A). The IgV-like domain of Ctla-4 was characterized by two-layer β-sandwich and was conserved between zebrafish and humans (Fig. 1B). Ctla-4 exists as a dimer, and unlike the intracellular localization of CTLA-4 in mammals, Ctla-4 was located on the cell membrane (Fig. 1C and D). Moreover, Ctla-4 was mainly expressed on the T cells, including the Cd4<sup>+</sup> T cells and Cd8<sup>+</sup> T cells (Fig. 1E and F).

### Ctla-4 deficiency induces inflammatory bowel disease (IBD)-like phenotype

To further investigate the function of Ctla-4, we generated a *ctla-4*<sup>-/-</sup> zebrafish line with a 14-base deletion in the second exon of the *ctla-4* gene (Fig. 2A–C). The zebrafish appeared grossly normal in appearance; however, the body weight and size were significantly reduced compared with those of wild-type zebrafish (Fig. 2D and E). Anatomically, the *ctla-4*<sup>-/-</sup> zebrafish were featured by intestine shortening and splenomegaly, suggesting the occurrence of chronic inflammation in the intestines (Fig. 2F and G). For clarification, we first performed histological analysis on the anterior, mid, and posterior intestine segments using H&E staining. Compared with the wild-type zebrafish, the *ctla-4*<sup>-/-</sup> fish exhibited significant epithelial hyperplasia in the anterior intestine segment, accompanied with a small amount of mucosal inflammatory cell infiltration (Fig. 2H). This result indicates an enhanced regeneration of the intestine, which is typically observed in cases of intestinal inflammation [22]. A noteworthy goblet cell loss which marks the severity of intestinal inflammation was also observed in *ctla-4*<sup>-/-</sup> anterior intestine, as quantified through PAS staining (Fig. 2I and J). Besides, a small amount of lymphocytic infiltration and mild epithelial damage occurred in the mid intestine segment of *ctla-4*<sup>-/-</sup> zebrafish (Fig. 2H). In posterior intestine of *ctla-4*<sup>-/-</sup> fish, the intestinal villi were markedly shortened, the epithelial barrier showed severely disrupted, and the intestinal wall became thinner, wherein the mucosal and transmural inflammatory cells were significantly infiltrated (Fig. 2H). Consistent with these observations, ultrastructure analysis revealed that the epithelial cells of posterior intestine in *ctla-4*<sup>-/-</sup> zebrafish exhibited alteration in tight junction, the loss of adhesion junctions and desmosomes, and disruption of microvilli (Fig. 2K). All these results strongly indicate that Ctla-4 plays a crucial role in preserving intestinal homeostasis in zebrafish. The intestinal phenotype resulting from Ctla-4 deficiency was similar to IBD in mammals.

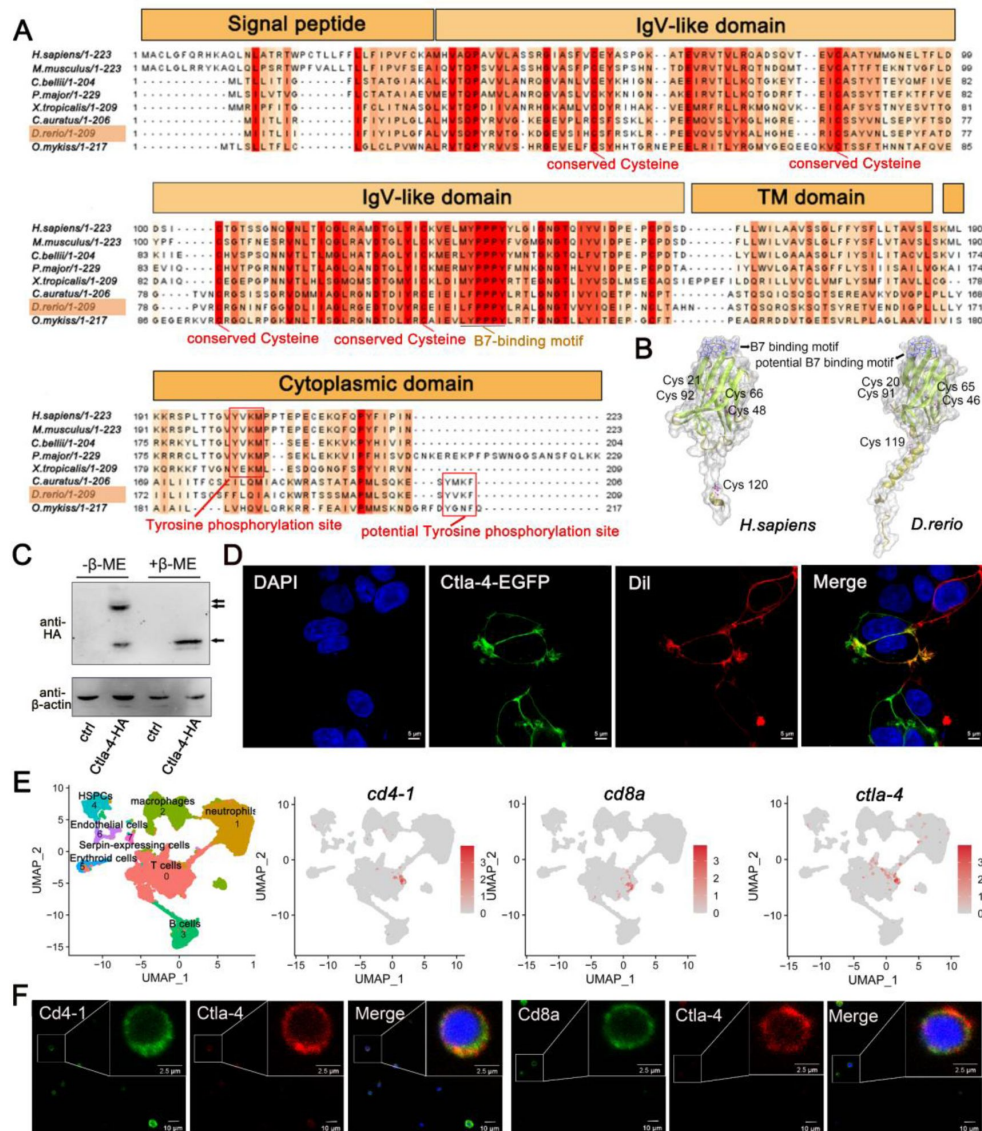


**Fig. 1**

Characterization of zebrafish Ctla-4. **A** Alignment of the Ctla-4 homologues from different species generated with ClustalX and Jalview. The conserved and partially conserved amino acid residues in each species are colored in hues graded from orange to red, respectively. The conserved Cysteine residues, and conserved functional motifs, such as B7-binding motif, Tyrosine phosphorylation site, and potential Tyrosine phosphorylation site were indicated separately. The signal peptide, IgV-like domain, transmembrane (TM) domain and cytoplasmic domain were marked at the top of the sequence. **B** Tertiary protein structures of Ctla-4 ectodomains between humans and zebrafish were predicted by AlphaFold2. The two pairs of disulfide bonds (Cys<sup>20</sup>-Cys<sup>91</sup>/Cys<sup>46</sup>-Cys<sup>65</sup> in zebrafish and Cys<sup>21</sup>-Cys<sup>92</sup>/Cys<sup>48</sup>-Cys<sup>66</sup> in humans) used to connect the two-layer  $\beta$ -sandwich, and the separate Cys residue (Cys<sup>119</sup> in zebrafish and Cys<sup>120</sup> in humans) associated with the dimerization of the proteins are indicated. The Cys residues are represented in purple ball-and-stick and the identified or potential B7 binding sites are highlighted in blue. **C** Dimer of Ctla-4 was identified by Western blot under reducing (+ $\beta$ -ME) or non-reducing (- $\beta$ -ME) conditions. The ctrl represents the empty control plasmid. The monomer is indicated by one arrow, the dimer by two arrows. **D** The subcellular localization of Ctla-4 protein was assessed in HEK293T cells transfected with pEGFPN1-Ctla-4 for 48 hours using a two-photon laser-scanning microscope (Original magnification, 630 $\times$ ). The nucleus was stained with DAPI (blue), the cell membrane was stained with DiI (red). **E** tSNE plots show the relative distribution of common T cell markers *cd4-1*, *cd8a* and *ctla-4*. The data are from splenic single cell RNA sequencing (scRNA-seq) dataset we recently established [59]. **F** Immunofluorescence staining of lymphocytes separated from blood, spleens, and kidneys of zebrafish. Cells were stained with mouse anti-Ctla-4, together with rabbit anti-Cd4-1 or rabbit anti-Cd8a. DAPI stain shows the location of the nuclei. The images were obtained by two-photon laser-scanning microscope (Original magnification, 630 $\times$ ).

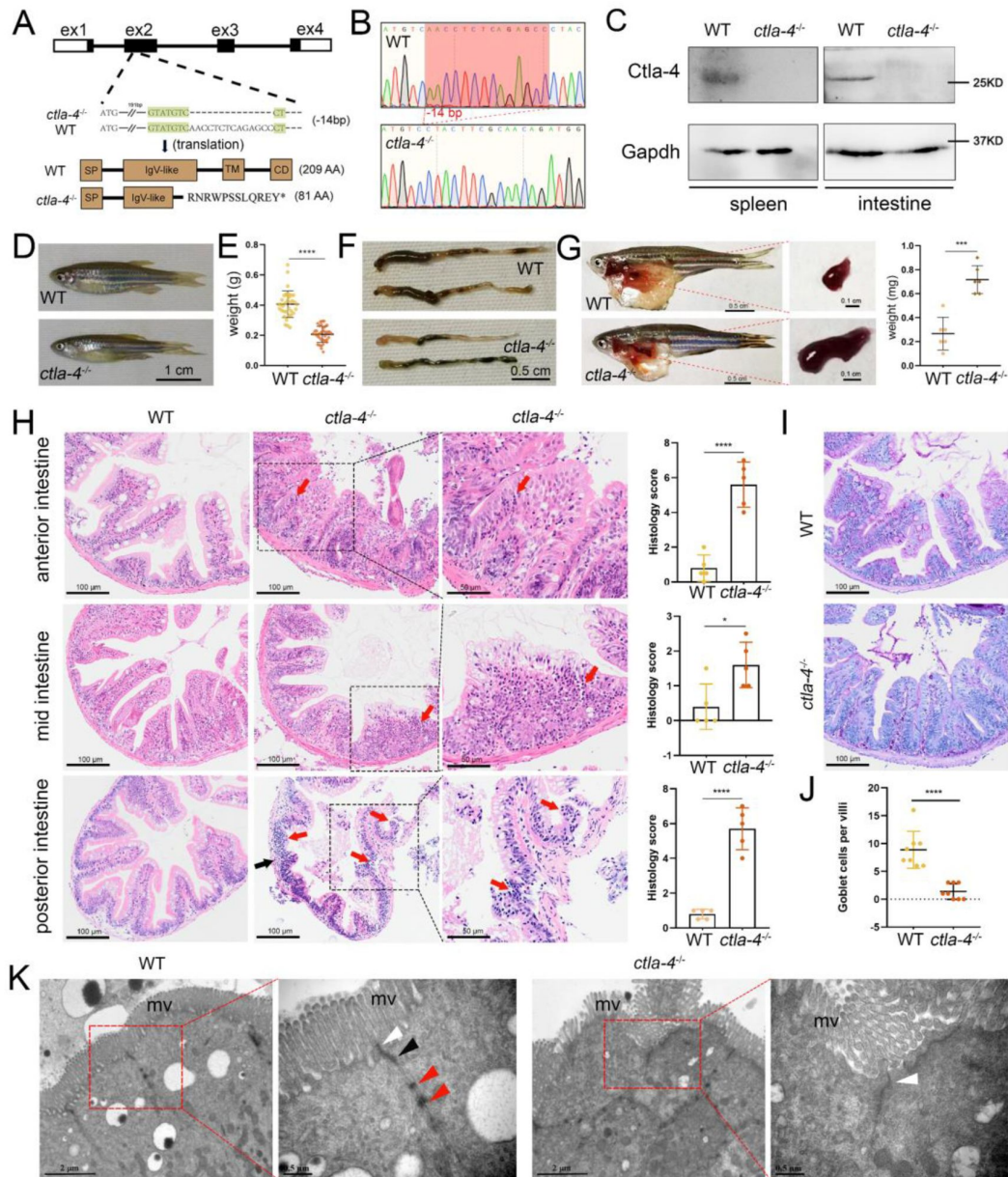


**Fig. 2**

Examination on the IBD-like phenotype in *ctla-4*<sup>-/-</sup> zebrafish. **A** Generation of a homozygous *ctla-4*-deficient (*ctla-4*<sup>-/-</sup>) zebrafish line through CRISPR/Cas9-based knockout of *ctla-4* gene on chromosome 9. A 14-bp deletion mutation in exon 2 results in a premature stop at codon 82, which is predicted to produce a defective Ctla-4 protein containing 81 amino acids. **B** Genotyping of the deficiency of *ctla-4* gene by Sanger sequencing. **C** Knockout efficiency of Ctla-4 selectively examined in spleen and gut tissues of *ctla-4*<sup>-/-</sup> zebrafish by Western blot analysis. Gapdh serves as a loading control. **D** Normal gross appearance of adult wild-type (WT) and *ctla-4*<sup>-/-</sup> zebrafish. **E** Body weight statistics of WT and *ctla-4*<sup>-/-</sup> zebrafish (n = 30). **F** The change of intestine length in WT and *ctla-4*<sup>-/-</sup> zebrafish. **G** The change of splenic size in WT and *ctla-4*<sup>-/-</sup> zebrafish. **H** Representative H & E staining analysis of histopathological changes and quantitation of histology score in anterior, mid and posterior intestines from WT and *ctla-4*<sup>-/-</sup> zebrafish. Red arrows indicate mucosal inflammatory cell infiltration, and black arrow indicates transmurial inflammatory cell infiltration. **I** PAS analysis indicates goblet cells in anterior intestine from WT and *ctla-4*<sup>-/-</sup> zebrafish. **J** Quantitation analysis of goblet cells of each villus in the foregut of WT and *ctla-4*<sup>-/-</sup> zebrafish (n = 8). **K** Observation of cell junctions between intestinal epithelial cells in posterior intestines from WT and *ctla-4*<sup>-/-</sup> zebrafish under TEM (Hitachi Model H-7650). White triangles indicate tight junctions, black triangle indicates adhesion junctions, and red triangles indicate desmosomes. Data are presented as mean ± standard deviation (SD). Statistical significance was assessed through an unpaired Student's t test (\*p < 0.05; \*\*p < 0.01; \*\*\*p < 0.001; \*\*\*\*p < 0.0001).

## Molecular mechanisms of Ctlα-4 deficiency-induced IBD-like phenotype

To explore the potential molecular mechanisms of Ctlα-4 deficiency-induced IBD-like phenotype, we performed transcriptome profiling analysis of intestines from wild-type and *ctlα-4*<sup>-/-</sup> zebrafish. We identified a total of 1,140 differentially expressed genes (DEGs), among which 714 genes were up-regulated, and 426 genes were down-regulated in *ctlα-4*<sup>-/-</sup> zebrafish (Fig. 3A and B). GO enrichment analysis showed that DEGs or up-regulated genes in the top 10 enriched biological processes were associated with the immune response and inflammatory response (Fig. 3C and D). Moreover, the KEGG enrichment analyses indicated that the up-regulated DEGs are primarily involved in the process of cytokine-cytokine receptor interaction and cell adhesion molecules, which are also related to inflammation (Fig. S3A); however, the down-regulated DEGs were significantly enriched in the process of metabolism (Fig. S3B). The intestines of *ctlα-4*<sup>-/-</sup> zebrafish showed significant upregulation of *il1b*, *tnfa*, myeloid-specific peroxidase (*mpx*), matrix metalloproteinase 9 (*mmp9*), chemokine (C-X-C motif) ligand 8a (*cxcl8a*), and *il13*, a Th2-typical cytokine crucial for ulcerative colitis in mammals [23]. In contrast, *il10*, a potent anti-inflammatory cytokine, was markedly down-regulated in Ctlα-4-deficient intestines (Fig. 3E). The transcriptional change of these genes was confirmed by RT-qPCR (Fig. 3F). By constructing the PPI network, we found that *il1b* was a major cytokine that played a hub role in promoting the bowel inflammation of *ctlα-4*<sup>-/-</sup> zebrafish (Fig. 3G). Moreover, Gene set enrichment analysis (GSEA) showed that genes involved in the lymphocyte chemotaxis, positive regulation of ERK1 and ERK2 cascade, Calcium and MAPK signaling pathways were positively enriched in *ctlα-4*<sup>-/-</sup> zebrafish intestines, implying a sensitized or activated state of lymphocytes due to the absence of Ctlα-4 (Fig. S3C and D). Notably, biological processes related to neutrophil activation and chemotaxis were significantly enriched (Fig. 3C and D). Studies have shown that neutrophils can induce histopathological effects through releasing matrix metalloproteinases (MMPs), neutrophil elastase, and myeloperoxidase (MPO) [24]. To confirm the association between neutrophils and Ctlα-4-deficient intestinal inflammation, the MPO level was examined. As a support, MPO activity was markedly increased in the intestines and peripheral blood of *ctlα-4*<sup>-/-</sup> zebrafish (Fig. 3H). Besides, a number of biological markers or susceptibility genes of IBD observed in mammals, including c-reactive protein 6 (*crp6*), *crp7*, MMPs, haptoglobin, *il23r*, insulin-like growth factor binding protein 1 a (*igfbp1a*), cAMP responsive element modulator b (*cremb*) and lymphocyte specific protein 1 b (*lsp1b*), were highly expressed in the *ctlα-4*<sup>-/-</sup> zebrafish (Fig. 3I and J) [9, 25, 26], suggesting the presence of a conserved molecular network underlying IBD pathogenesis between *ctlα-4*<sup>-/-</sup> zebrafish and mammalian models.

## Cellular mechanisms of Ctlα-4 deficiency-induced IBD-like phenotype

To investigate the cellular mechanisms underlying the IBD-like phenotype induced by Ctlα-4 deficiency, we performed scRNA-seq analysis on intestines from wild-type and *ctlα-4*<sup>-/-</sup> zebrafish using the 10× Genomics Chromium platform. We obtained nine discrete clusters from 7,539 cells of wild-type and *ctlα-4*<sup>-/-</sup> zebrafish (Fig. 4A). These clusters of cells were classified as enterocytes, enteroendocrine cells, smooth muscle cells, neutrophils, macrophages, B cells, and a group of T/NK/ILC-like cells based on their co-expression of lineage marker genes (Fig. 4B and C, Fig. S4A and B). Due to severe epithelial disruption and inflammatory cell infiltration in *ctlα-4*<sup>-/-</sup> zebrafish intestines, we focus on the pathological process and immune reactions in enterocytes and immune cell populations. KEGG analysis showed that apoptotic pathway was highly enriched in enterocytes of *ctlα-4*<sup>-/-</sup> zebrafish, suggesting that aberrant apoptosis contributes to the epithelial injury (Fig. S4C). Additionally, genes functionally involved in the formation of tight and adhesion junctions, such as *oclna*, *cdh1*, *pcdh1b* and *cldn15a*, were significantly down-regulated in enterocytes of *ctlα-4*<sup>-/-</sup> zebrafish (Fig. 4D), consistent with the pathological observation under

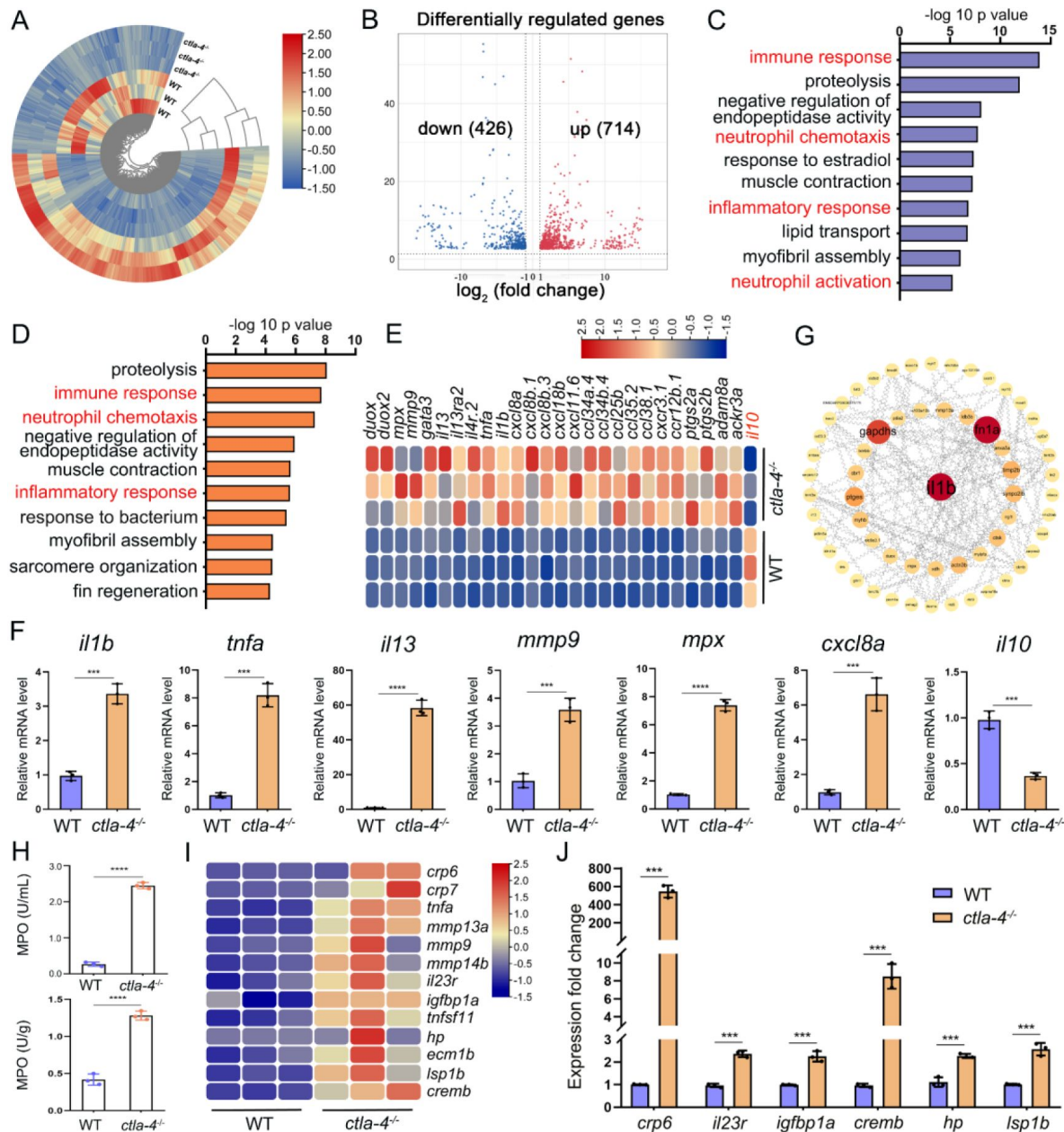


**Fig. 3**

RNA-sequencing analysis of the molecular implications associated with the IBD-like phenotype in *ctla-4*<sup>-/-</sup> zebrafish. **A** Heatmap of different expressed genes between the intestines from wild-type (WT) and *ctla-4*<sup>-/-</sup> zebrafish. **B** Volcano plot showing the up-/down-regulated genes in the intestines of *ctla-4*<sup>-/-</sup> zebrafish compared with those of WT zebrafish. Red indicates up-regulated genes and blue indicates down-regulated genes. **C** GO analysis showing top 10 terms in biological processes of DEGs. **D** GO analysis showing top 10 terms in biological processes of all up-regulated genes. **E** Heatmap of representative differently expressed inflammation and chemotaxis-related genes. **F** The mRNA expression levels of important genes associated with inflammation and chemokines confirmed by real-time qPCR. **G** Protein-protein interaction network was constructed using the DEGs. The nodes represent the proteins (genes); the edges represent the interaction of proteins (genes). **H** The MPO activity in the intestines (up) and peripheral blood (down). **I** Heatmap of IBD biomarker genes and IBD-related genes. **J** The mRNA expression levels of representative IBD biomarker genes and IBD-related genes were analyzed by real-time qPCR. Data are presented as mean  $\pm$  standard deviation (SD). Statistical significance was assessed through an unpaired Student's *t* test (\*\**p* < 0.01; \*\*\**p* < 0.001; \*\*\*\**p* < 0.0001).

electron microscope. Furthermore, inflammation-related genes and pathways were significantly up-regulated and enriched in neutrophils, B cells, and macrophages of *ctla-4<sup>-/-</sup>* zebrafish, suggesting active inflammatory responses (Fig. 4E-G, Fig. S4D). By sub-clustering analysis, six subpopulations were classified from T/NK/ILC-like cell groups based on their expression with a set of marker genes. These subpopulations include Cd8<sup>+</sup> T cells, ILC3-like cells, maturing Ccr7<sup>high</sup> T cells, NKT cells, and two groups of Th2 cells (Fig. 5A-C; Fig. S5A). The abundances of NKT and two subsets of Th2 cells were significantly increased in the intestines of *ctla-4<sup>-/-</sup>* zebrafish (Fig. 5D-F). These cells exhibited high expression of *il13*, a key contributor to intestinal inflammation in mammals (Fig. 5G and H) [23]. Specifically, the second subset of Th2 cells was seldom observed in the intestine of wild-type zebrafish, indicating their unique role in the pathogenesis of IBD-like phenotype in *ctla-4<sup>-/-</sup>* zebrafish (Fig. 5D-F). KEGG analysis of up-regulated genes from *ctla-4<sup>-/-</sup>* NKT and Th2 cells indicated that Ctla-4 deficiency is positively associated with the inflammatory cytokine-cytokine receptor interaction, PPAR, calcium and MAPK signaling pathways, cellular adhesion and mucosal immune responses (Fig. 5I and J; Fig. S5B), suggesting high activity of NKT and Th2 cells in inflamed intestines [27, 28]. Although the abundance of Cd8<sup>+</sup> T cells was not significantly changed in Ctla-4-deficient intestines, the inflammatory genes and pathways were up-regulated and enriched in the subset of T cells (Fig. S5C and D). Notably, the proportion of ILC3-like cells was decreased, and they highly expressed *il17a/f1* and *il17a/f3* in the Ctla-4-deficient intestines (Fig. 5D-F, and K). Investigations have consistently reported a substantial decline in the population of ILC3s within the inflamed intestines and IL-17A-secreting ILC3s play a significant role in the development of intestinal inflammation [29–34]. Thus, the reduced ILC3-like cells and increased expression of *il17a/f1* and *il17a/f3* may be responsible for intestinal inflammation induced by Ctla-4 deficiency.

## Decreased microbiota diversity in *ctla-4<sup>-/-</sup>* zebrafish intestines

The intestinal microbiota plays a crucial role in host functions such as nutrient acquisition, metabolism, epithelial cell development and immunity. Notably, lower microbiota diversity has consistently been observed in patients with IBD phenotype [35, 36], making it a valuable indicator of host health. Therefore, we further analyzed whether microbes are involved in the Ctla-4-deficiency induced intestinal inflammation. The results revealed a significantly higher number of amplicon sequence variants (ASVs) in wild-type zebrafish intestines, with 730 ASVs unique to the wild-type group and 276 ASVs exclusively found in *ctla-4<sup>-/-</sup>* group (Fig. 6A). Furthermore, the Shannon index and the Simpson index indicated a decreased microbial diversity in *ctla-4<sup>-/-</sup>* zebrafish intestines (Fig. 6B) and the Principal Coordinate Analysis (PCoA) using Bray Curtis distance revealed a significant separation in the microbial composition between *ctla-4<sup>-/-</sup>* group and the wild-type group (Fig. 6C). To gain insights into the microbial community composition, we analyzed the identified microbial populations at the class and family level. Alphaproteobacteria and Gammaproteobacteria were found to be the most prevalent classes. Relative to wild-type group, Ctla-4 deficiency resulted in a significant reduction in Alphaproteobacteria abundance. However, the Gammaproteobacteria, one of the main classes of Gamma-negative pathogenic bacteria expanded under inflammation conditions, was increased, although the change did not reach statistical significance (Fig. 6D and E) [37]. In addition, we observed a decreased relative abundance of short-chain fatty acids (SCFAs)-producing Bacilli and Verrucomicrobiae, the latter of which contributes to glucose homeostasis and intestinal health (Fig. 6F and G) [38, 39]. Notably, the family-level analysis revealed a notable enrichment of Enterobacteriaceae, overgrowing under host inflammatory conditions, and the Shewanellaceae, serving as the most important secondary or opportunistic pathogens, in *ctla-4<sup>-/-</sup>* zebrafish (Fig. 6H and I). To identify differentially abundant bacterial taxa between the wild-type and *ctla-4<sup>-/-</sup>* zebrafish, we conducted Linear discriminant analysis (LDA) effect size (LEfSe). The results showed that several potentially opportunistic pathogens, including Gammaproteobacteria, Enterobacteriales, and Aeromonadales were found to be overrepresented in *ctla-4<sup>-/-</sup>* zebrafish (Fig. 6J). In contrast, Actinobacteriota, Cetobacterium, and Planctomycetota (Planctomycetes) were

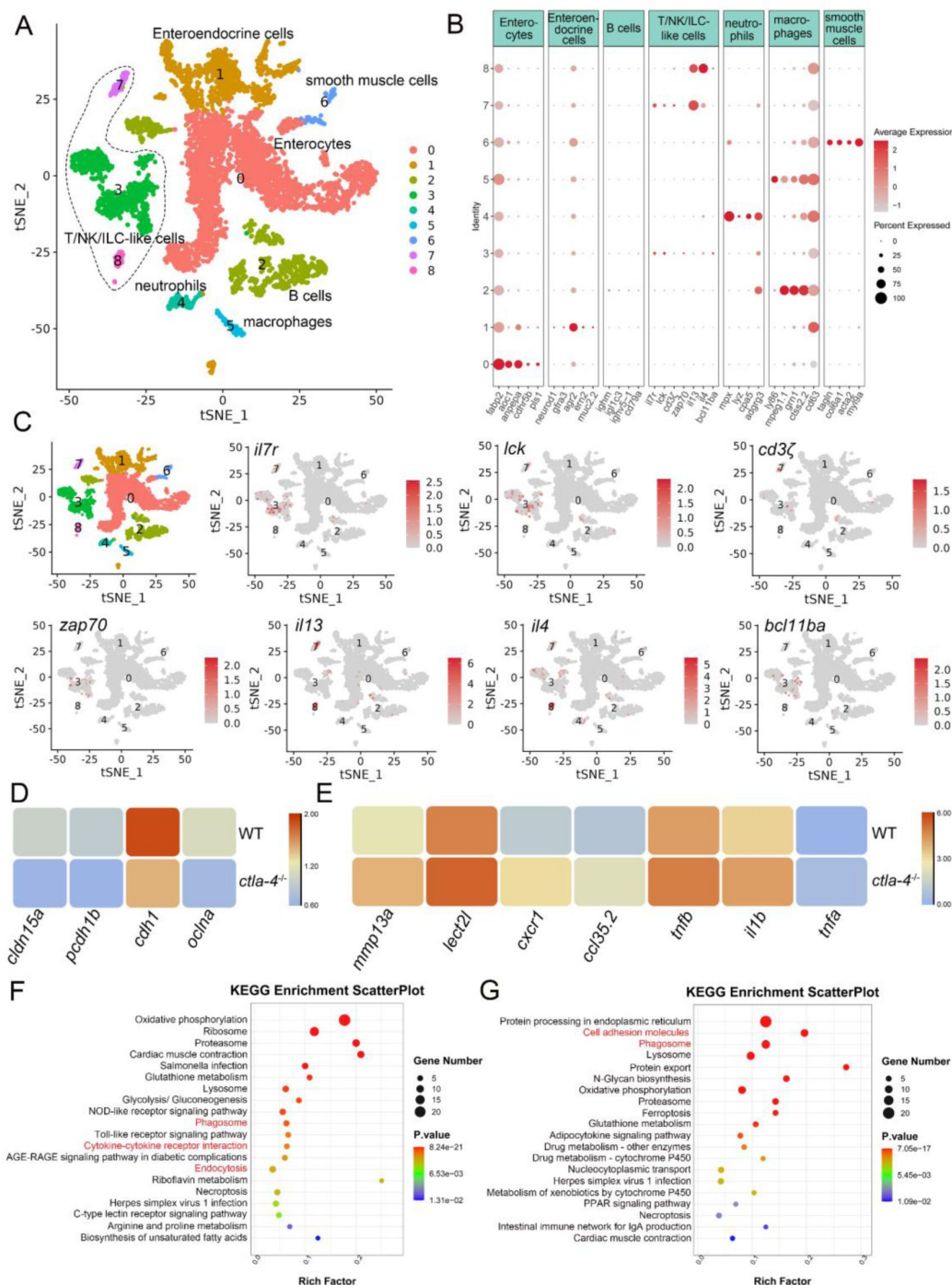


**Fig. 4**

Single cell RNA-sequencing analysis of the major cell types associated with the IBD-like phenotype in *ctla-4<sup>-/-</sup>* zebrafish. **A** Classification of cell types from zebrafish intestines by tSNE nonlinear clustering. **B** Dot plot showing the expression levels of lineage marker genes and percentage of cells per cluster that express the gene of interest. **C** Expression maps of T cell associated markers within the cell populations of the zebrafish intestines. **D** Heatmap of the tight/adhesion junction-related genes in enterocytes among the samples from wild-type (WT) and *ctla-4<sup>-/-</sup>* zebrafish. **E** Heatmap of inflammation-related genes involved in cytokine-cytokine receptor interaction in neutrophils among the samples from WT and *ctla-4<sup>-/-</sup>* zebrafish. **F** KEGG enrichment analysis showing the top 15 terms of up-regulated genes in neutrophils from the *ctla-4<sup>-/-</sup>* sample versus the WT sample. **G** KEGG enrichment analysis showing the top 15 terms of up-regulated genes in macrophages from the *ctla-4<sup>-/-</sup>* sample versus the WT sample.

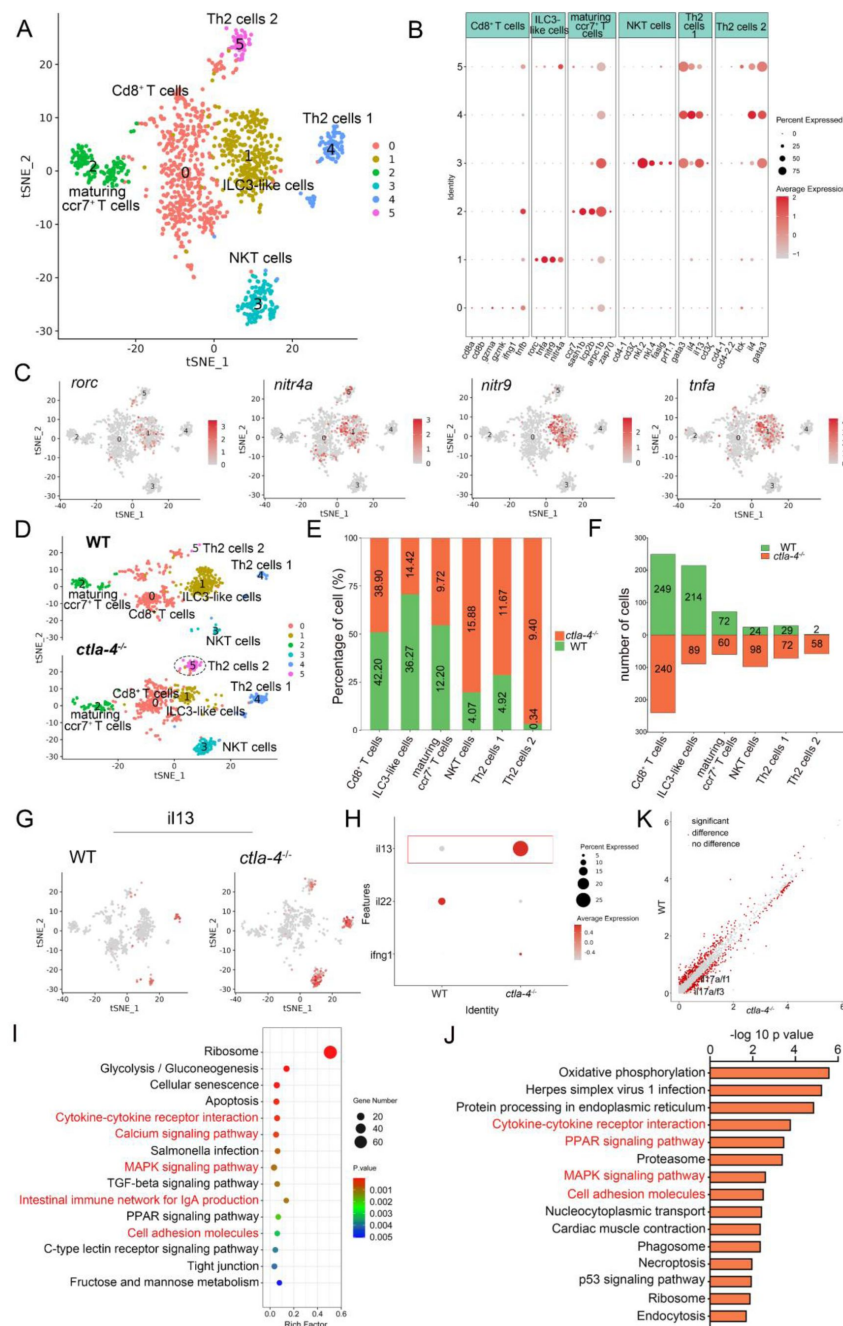


**Fig. 5**

Single cell RNA-sequencing analysis of the subset immune-cells associated with the IBD-like phenotype in *ctla-4*<sup>-/-</sup> zebrafish. **A** Classification of subset cells from the T/NK/ILC-like group by tSNE nonlinear clustering. **B** Dot plot showing the expression levels of subset marker genes and percentage of cells per cluster that express the gene of interest. **C** Marker gene expression in individual cluster identifying this cluster as ILC3-like cells. **D** Changes in the composition of subset cells between samples from wild-type (WT) and *ctla-4*<sup>-/-</sup> zebrafish. A significantly increased Th2 subset (referred to as Th2 cells 2) in the *ctla-4*<sup>-/-</sup> sample was highlighted with a black dashed circle. **E** Histogram showing the different ratios of subset cells between the WT and *ctla-4*<sup>-/-</sup> samples. **F** Histogram presenting the different numbers of subset cells between the WT and *ctla-4*<sup>-/-</sup> samples. **G** Expression maps of the cytokine *il13* within different subset cells between the WT and *ctla-4*<sup>-/-</sup> samples. **H** Dot plots illustrating the differential expression of *il13* in T/NK/ILC-like cells from WT and *ctla-4*<sup>-/-</sup> zebrafish. **I** KEGG enrichment analysis showing the top 15 terms of up-regulated genes in the subset of Th2 cells 2. **J** KEGG enrichment analysis showing the top 15 terms of up-regulated genes in NKT cells. **K** Scatter plot showing the DEGs of ILC3-like cells in WT and *ctla-4*<sup>-/-</sup> zebrafish. The *il17a/f1* and *il17a/f3* was shown in the scatter plot.

more abundant in the wild-type zebrafish. These findings strongly indicated an association between Ctla-4 deficiency-induced gut inflammation and dysbiosis, as characterized by decreased microbial diversity, loss of potentially beneficial bacteria, and expansion of pathobionts.

## Inhibitory role of Ctla-4 in T cell activation

Given that Ctla-4 is primarily expressed on T cells (Fig. 1E–F), and its absence has been shown to result in intestinal immune dysregulation, indicating a crucial role of this molecule as a conserved immune checkpoint in T cell inhibition. For clarification, the lymphocyte proliferation was examined by a series of blockade/inhibition assays using anti-Ctla-4 Ab, recombinant soluble Ctla-4-Ig (sCtla-4-Ig), sCd28-Ig, and sCd80/86 proteins in a PHA-stimulating and mixed lymphocyte reaction (MLR) model (Fig. S6 A–C). Results showed that the lymphocyte proliferation was more pronounced in the absence of Ctla-4, and the supplementation of sCtla-4-Ig inhibited cell proliferation, suggesting the inhibitory function of Ctla-4 in T cells (Fig. 7A and B). Consistent with these results, blockade of Ctla-4 by administering anti-Ctla-4 Ab significantly promoted the proliferation of lymphocytes from wild-type zebrafish (Fig. 7C). Moreover, administration of sCd28-Ig into the co-cultures also inhibited the proliferation of lymphocytes from *ctla-4*<sup>-/-</sup> zebrafish (Fig. 7D). Besides, the addition of Cd80/86 significantly promoted the expansion of Ctla-4-deficient lymphocytes (Fig. 7E). Based on these results, we concluded that the presence of Ctla-4 obstructs the Cd80/86–Cd28 mediated costimulatory signaling, consequently impeding cell proliferation. To further investigate the relationship between Cd28, Ctla-4 and Cd80/86, we assessed the interaction between these molecules *in vitro*. Our bioinformatics analysis by AlphaFold2, flow cytometry and Co-IP assays demonstrated the interaction between Cd28/Ctla-4 and Cd80/86 (Fig. 7F–H, Fig. S6D). Moreover, using a microscale thermophoresis assay, we found that Ctla-4 has higher affinity for Cd80/86 than Cd28, as indicated by a lower equilibrium association constant value ( $K_D = 0.50 \pm 0.25 \mu\text{M}$  vs.  $K_D = 2.64 \pm 0.45 \mu\text{M}$ ) (Fig. 7I). These results suggested that Ctla-4 could exert its inhibitory function by competing with Cd28 for binding Cd80/86.

## sCtla-4-Ig alleviates IBD-like phenotype

As described above, engagement of Cd80/86 by sCtla-4-Ig effectively suppressed T cell activation *in vitro* (Fig. 7B), indicating that sCtla-4-Ig holds promise as a potential intervention for IBD-like phenotype. This is supported by the observation that zebrafish treated with sCtla-4-Ig exhibited obvious body weight restoration compared to those treated with the IgG isotype control (Fig. 8A). To provide further evidence, histological analysis was performed on the posterior intestine, which is known to experience severe tissue destruction under Ctla-4 deficient conditions. As expected, Ctla-4-Ig treatment resulted in a significant decrease in lymphocyte infiltration and an improvement in the epithelial barrier (Fig. 8B). Moreover, Ctla-4-Ig treatment significantly reduced the expression of pro-inflammatory genes, including *il13*, *tnfa*, *mpx*, *mmp9*, and *cxcl8a*, as well as *igfbp1a*, *cremb*, and *lsp1a*, which are susceptibility genes for IBD observed in mammals (Fig. 8C and D). These findings demonstrate that the supplementation of Ctla-4-Ig alleviates intestinal inflammation in Ctla-4-deficient zebrafish, highlighting its potential as a therapeutic intervention for CTLA-4 deficiency-induced IBD in mammals.

## Discussion

As an essential negative regulator of T cell activation, dysfunction of CTLA-4 was implicated in various diseases in both humans and murine models [40–42]. Numerous previous studies have established the connection between CTLA-4 and autoimmune thyroiditis, Graves' disease, myocarditis, pancreatitis, multiple sclerosis, rheumatoid arthritis, and type I diabetes [43–49]. However, the involvement of CTLA-4 in IBD has been understudied. Several investigations



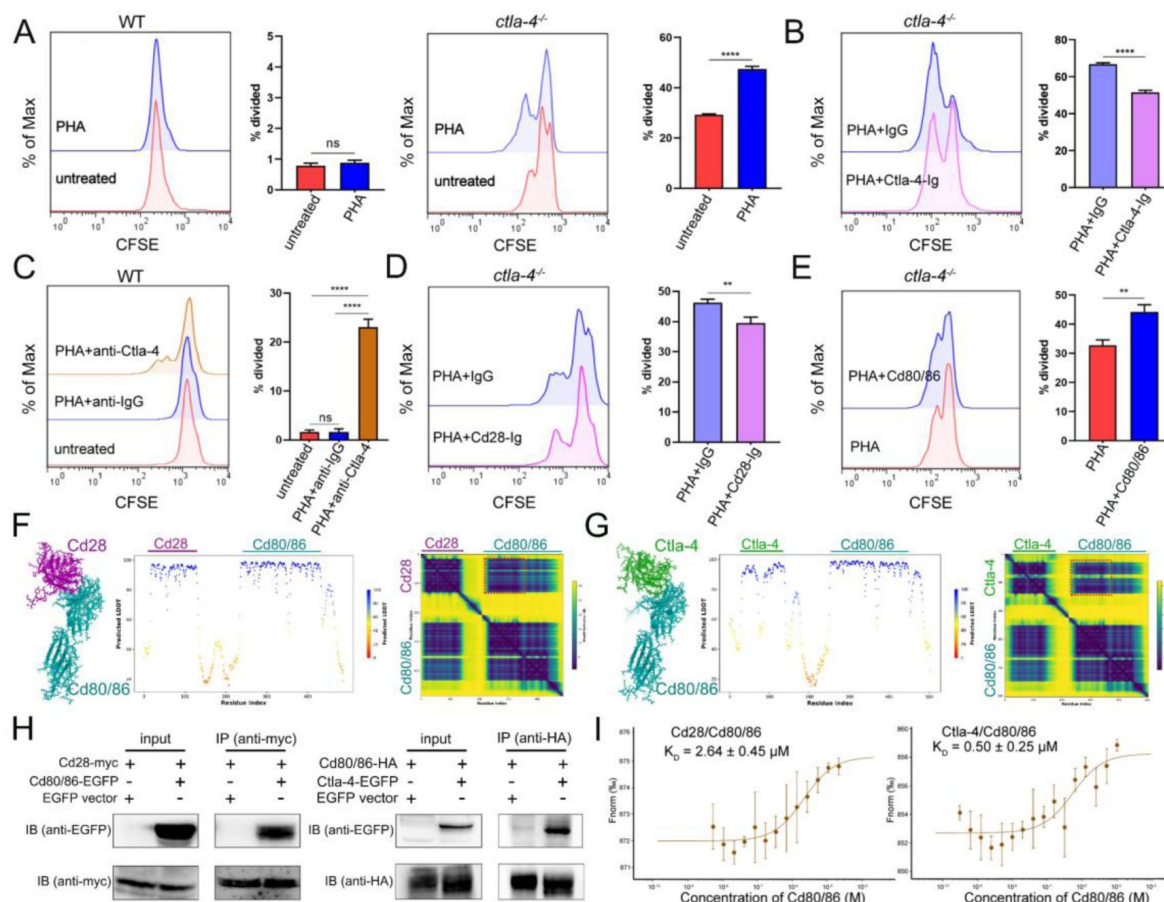


**Fig. 7**

Examination on the inhibitory function of Ctla-4 in T cell activation. **A** Assessment of the proliferative activity of T cells from wild-type and *ctla-4*<sup>-/-</sup> zebrafish by a mixed lymphocyte reaction combined with PHA-stimulation. The CFSE dilution, which served as an indicator of lymphocyte proliferation, was measured through flow cytometry. **B** Assessment of the proliferative activity of lymphocytes from *ctla-4*<sup>-/-</sup> zebrafish by the administration of sCtla-4-Ig. **C** Assessment of the proliferative activity of lymphocytes from wild-type zebrafish by supplementing anti-Ctla-4 antibody. **D** Assessment of the proliferative activity of lymphocytes from *ctla-4*<sup>-/-</sup> zebrafish by the administration of sCd28-Ig. **E** Assessment of the proliferative activity of lymphocytes from *ctla-4*<sup>-/-</sup> zebrafish by the administration of recombinant Cd80/86 protein. **F, G** Interactions between Cd80/86 and Cd28 (**F**), and Cd80/86 and Ctla-4 (**G**) as predicted by AlphaFold2. On the left are structural models depicting Cd80/86 in complex with Cd28 or Ctla-4. The center panels display per-residue model confidence scores (pLDDT) for each structure, using a color gradient from 0 to 100, where higher scores indicate increased confidence. The right panels show the predicated aligned error (PAE) scores for each model. The well-defined interfaces between Cd28 or Ctla-4 and Cd80/86 are highlighted with red dashed squares. **H** The interaction between Cd80/86 and Cd28 (left), and Cd80/86 and Ctla-4 (right) were verified by Co-IP. **I** Binding affinities of the Cd80/86 protein for the Cd28 and Ctla-4 proteins were measured by the MST assay. The  $K_D$  values are provided. Data are presented as mean  $\pm$  standard deviation (SD), which were calculated from three independent experiments. Statistical significance was assessed through an unpaired Student's t test (\*\* $p < 0.01$ ; \*\*\* $p < 0.001$ ; ns denotes no statistical significance).

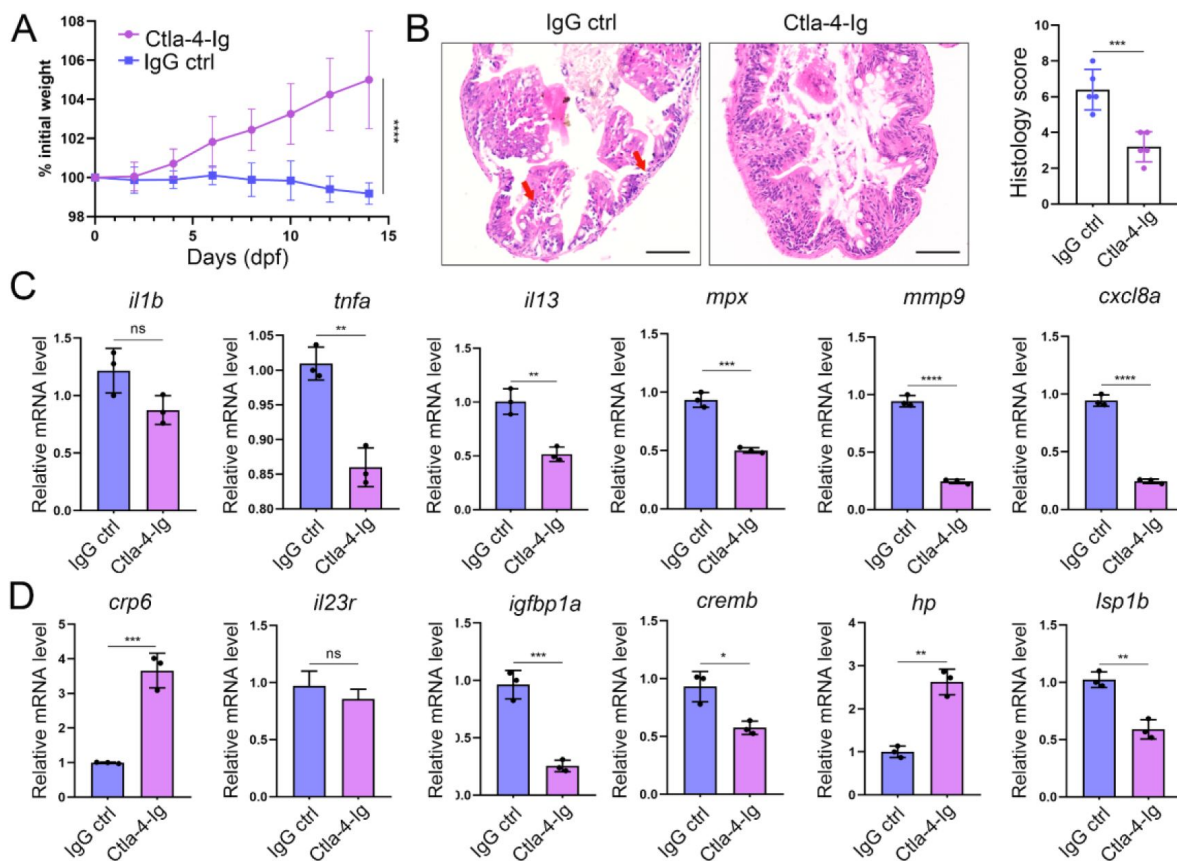


**Fig. 8**

In vivo inhibition of intestinal inflammation by Ctla-4-Ig. **A** Percent initial weight of zebrafish after injection of the Ctla-4-Ig or the IgG isotype control. In each group,  $n = 6$ . Data show means with SEM analyzed by two-way ANOVA with Sidak's correction for multiple comparisons. **B** Representative H&E staining analysis of histopathological changes and quantitation of histology score in the posterior intestine from Ctla-4-Ig or IgG isotype control-supplemented *ctla-4*<sup>-/-</sup> zebrafish. Scale bar: 50  $\mu$ m. **C** The mRNA expression levels of inflammation-related genes in the Ctla-4-Ig or IgG isotype control treatment groups of *ctla-4*<sup>-/-</sup> zebrafish. **D** The mRNA expression levels of IBD biomarker genes and IBD-related genes in the Ctla-4-Ig or IgG isotype control treatment groups of *ctla-4*<sup>-/-</sup> zebrafish. The  $p$  value was generated by unpaired two-tailed Student's  $t$ -test. \*\* $p < 0.01$ ; \*\*\* $p < 0.001$ ; \*\*\*\* $p < 0.0001$ .

have reported that haploinsufficiency resulting from mutations in CTLA-4 in humans is associated with IBD, and genome-wide association studies (GWAS) have implicated CTLA-4 as a susceptibility gene for IBD [50–52]. Nevertheless, the exact contributions and mechanisms of CTLA-4 deficiency in the occurrence and pathology of IBD remain incompletely understood, primarily due to the lack of animal models attributable to the lethality of CTLA-4 knockout in mice. In this study, we identified the *Ctla-4* homolog in zebrafish, and discovered that defect in *Ctla-4* did not have a severe lethal effect, but did show a clear IBD-like phenotype. This makes zebrafish an attractive animal model for investigating the molecular and cellular mechanisms underlying *Ctla-4* mediated IBD. Multiple lines of experimental evidence demonstrated the IBD-like phenotype in *Ctla-4*-deficient zebrafish. These include the observed destruction of epithelial integrity and infiltration of inflammatory cells in the inflamed intestines during histopathological analysis, the enrichment of inflammation-related pathways and the imbalance between pro-inflammatory and anti-inflammatory cytokines identified through transcriptome profiling, the abnormal composition of immune cell populations revealed by single-cell RNA sequencing, as well as the reduced diversity and altered composition of intestinal microbiota. These observations collectively suggest that *Ctla-4* may serve as a potential genetic determinant of the IBD-like phenotype, although further research is required to definitively identify the causative variant responsible for this association. Moreover, the establishment of zebrafish models provides a valuable tool for comprehending the underlying mechanisms of the disease's pathophysiology.

A multi-omics study was conducted to investigate the mechanisms of *Ctla-4*-deficiency induced IBD. RNA-seq analysis demonstrated a significant upregulation of important inflammatory cytokines, such as *il1b* and *tnfa* in the *Ctla-4*-deficient intestines. This is consistent with studies showing that IL-1 $\beta$  and TNF- $\alpha$  act as crucial mediators in mammalian IBD models by disrupting epithelial junctions and inducing apoptosis of epithelial cells [53, 54]. Conversely, the key anti-inflammatory cytokines, such as *il10*, were downregulated. These findings highlight an imbalance between pro-inflammatory and anti-inflammatory cytokines in the intestines of *Ctla-4*-deficient fish. Consistently, the inflammatory signaling pathways associated with these upregulated cytokines, such as the ERK1/2 and MAPK pathways, were positively enriched in inflamed intestines. Single-cell RNA-seq analysis revealed the upregulation and enrichment of these inflammatory cytokines and pathways in neutrophils, macrophages, and B cells of inflamed intestines, indicating their active involvement in inflammatory responses and as major sources of inflammatory signals. Additionally, there was a marked increase in the abundance of Th2 subset cells in the inflamed intestines. These Th2 cells exhibited high expression of *il13* and were significantly enriched in inflammatory signaling pathways, indicating their activated state. Previous research in mammals has identified IL-13 as the key effector Th2 cytokine in ulcerative colitis, directly causing damage to epithelial cells by affecting epithelial tight junctions, apoptosis, and cell restitution [23]. Therefore, upregulated IL13 from Th2 cells may be a significant contributor to epithelial injury in zebrafish model. Notably, the proportion of ILC3-like cells was downregulated in the inflamed intestines, consistent with recent studies reporting a substantial decline of ILC3 in IBD patients [29–31]. ILC3 is the most abundant type of ILCs in the intestines and plays a protective role in IBD in mammals by promoting epithelial cell proliferation and survival, as well as enhancing intestinal barrier function through the production of IL-22 [32, 34]. Thus, the marked decrease in ILC3-like cells may exacerbate intestinal inflammation and damage. Besides, abnormal activation of Th2 cells can lead to dysfunction in downstream B cells and mucosa-associated immunity, which is essential in maintaining the symbiotic bacterial homeostasis in intestines [38]. Thus, a potential correlation may exist between changes in Th2 cells and the observed alterations in the intestinal microbial community in *Ctla-4*-deficient zebrafish. Overall, our findings provided insights into the occurrence of IBD. However, gaining a comprehensive understanding of the complex interactions among these immune cells, intestinal epithelial cells, and the microbiome in IBD requires further exploration.

## Materials and Methods

### Experimental fish

Wild-type AB zebrafish (*D rerio*) of both sexes, 4–6 months of age with body weights ranging from 0.3 to 0.8 g and lengths of 3–4 cm, were reared in the laboratory in recirculating water at 26–28 °C under standard conditions as previously described [55]. All animal experiments were performed in accordance with legal regulations and were approved by the Research Ethics Committee of Zhejiang University.

### Generation of *Ctla-4*-deficient zebrafish

CRISPR/Cas9 system was used to knock out the *ctla-4* gene. The targeting sequence 5'-CTCAGAGCCCTACTTCGCAA-3' was designed by optimized CRISPR Design (<http://crispr.mit.edu/>) and synthesized by T7 RNA polymerase and purified by MEGAclean Kit (AM1908; Invitrogen) *in vitro*. Cas9 protein (500 ng/μl, A45220P; Thermo Fisher Scientific) and purified RNA (90 ng/μl) were coinjected into one cell-stage wild-type embryos. For genotyping, DNA fragment was amplified with primers (F: 5'-TGTGACAGGAAAAGATGGAGAA-3' and R: 5'-GATCAGATCCACTCCTCCAAAG-3') and subjected to sequencing. The mutant alleles (~14 bp) were obtained and their offspring were used in experiments.

### Histopathological analysis

The anterior, mid, and posterior intestines (n = 3 replicates) were fixed in 4% PFA overnight and embedded in paraffin. The tissues were cut into 4 μm sections and stained with Hematoxylin and eosin (H&E) for pathological analysis. To evaluate the severity of intestinal inflammation, histologic scores were determined according to the criteria supplied by previous publication [22]. Briefly, three independent parameters, including inflammation, extent, and epithelial changes, were assessed and scored as follows: the severity of inflammation (0 = none, 1 = minimal, 2 = mild, 3 = moderate, 4 = marked); the level of inflammation extent (0 = none, 1 = mucosa, 2 = mucosa and submucosa, 3 = transmural), the degree of epithelial changes (0 = none, 1 = minimal hyperplasia, 2 = mild hyperplasia, minimal goblet cell loss, 3 = moderate hyperplasia, mild goblet cell loss, 4 = marked hyperplasia with moderate to marked goblet cell loss). Each parameter was calculated and summed to obtain the overall score. The sections were stained with Periodic Acid-Schiff (PAS) reagent to evaluate the number of goblet cells.

### RNA-sequencing and bioinformatic analysis

Total RNAs were isolated from wild-type or *ctla-4*<sup>-/-</sup> intestines (three biological replicates) using TRIzol reagent following the manufacturer's instructions (Takara). cDNA libraries were constructed using NEB Next Ultra Directional RNA Library Prep Kit (NEB), and sequencing was performed according to the Illumina HiSeq2500 standard protocol at LC Bio (Hangzhou, China). The differentially expressed genes (DEGs) were identified with absolute Log<sub>2</sub> fold change > 1 and adjusted *p*-value < 0.05 by R package DESeq2. Gene Ontology (GO) enrichment and Kyoto encyclopedia of genes and genomes (KEGG) enrichment analyses were performed by the OmicStudio (<http://www.omicstudio.cn/tool>) tools. Gene-set enrichment analysis was performed using software GSEA (v4.1.0, <https://www.gsea-msigdb.org/gsea/index.jsp>), and the heatmap was generated using the R package ggplot2. For the protein-protein interaction (PPI) networks, the DEGs were retrieved in STRING (version 11.5, <https://string-db.org/>) database (combined score > 0.4), and the PPI network was visualized by Cytoscape software (version 3.9.1) [56]. The betweenness centrality (BC) was calculated using the CytoNCA plugin in Cytoscape software. The RNA-sequencing (RNA-seq) data in this study were deposited in the Gene Expression Omnibus (GEO) (<http://www.ncbi.nlm.nih.gov/geo/>) database.

## Quantitative real-time PCR

Total RNA from intestines was extracted using TRIzol reagent (Takara Bio) and reverse transcribed into cDNAs according to the manufacturer's protocol. PCR experiments were performed in a total volume of 10  $\mu$ l by using an SYBR Premix Ex Taq kit (Takara Bio). The reaction mixtures were incubated for 2 min at 95°C, then subjected to 40 cycles of 15 s at 95°C, 15 s at 60°C, and 20 s at 72°C. Relative expression levels of the target genes were calculated using the  $2^{-\Delta\Delta Ct}$  method with  $\beta$ -actin for normalization. Each PCR trial was run in triplicate parallel reactions and repeated three times. The primers used in the experiments are listed in Supplemental Table 1.

## Single-cell RNA-sequencing analysis

The intestines from wild-type and *ctla-4*<sup>-/-</sup> zebrafish were washed by D-Hank's and incubated with D-Hank's containing EDTA (0.37 mg/mL) and DTT (0.14 mg/mL) for 20 min. The resulting supernatants were collected as fraction 1. The remaining tissues were subsequently digested with type IV collagenase (0.15 mg/mL) for 1 h at room temperature and the resulting supernatants were collected as fraction 2. Fractions 1 and 2 were combined and centrifuged at 350 g for 10 min. Cells were then washed with D-Hank's and suspended in 40% percoll (percoll : FBS: L-15 medium = 4 : 1: 5) and passed through a 40- $\mu$ m strainer. The cell suspension was carefully layered onto 63% percoll (percoll : FBS : L-15 medium = 6.3 : 1: 2.7) and centrifuged at 400 g for 30 min at room temperature. The cell layer of the interface was collected and washed with D-Hank's at 400 g for 10 min. Cell quantity and viability were assessed using 0.4% trypan blue staining, revealing that over 90% of the cells were viable. Single-cell samples were submitted to the LC-Bio Technology Co., Ltd (Hangzhou, China) for 10 $\times$  Genomics library preparation and data analysis assistance. Libraries were prepared using the Chromium<sup>TM</sup> Controller and Chromium<sup>TM</sup> Single Cell 3' Library & Gel Bead Kit v2 (10 $\times$  Genomics) according to the manufacturer's protocol, and sequenced on an Illumina NovaSeq 6000 sequencing system (paired-end multiplexing run, 150 bp) at a minimum depth of 20,000 reads per cell. Sequencing results were demultiplexed and converted to FASTQ format using Illumina bcl2fastq software and the data were aligned to Ensembl zebrafish genome assembly GRCz11. Quality control was performed using the Seurat. DoubletFinder R package was used to identify and filter the doublets (multiplets) [57]. The cells were removed if they expressed fewer than 500 unique genes, or > 60% mitochondrial reads. The number of cells after filtration in the current study was 3,263 in wild-type and 4,276 in *ctla-4*<sup>-/-</sup> groups, respectively. Cells were grouped into an optimal number of clusters for *de novo* cell type discovery using Seurat's FindNeighbors() and FindClusters() functions, graph-based clustering approach with visualization of cells being achieved through the use of t-SNE or UMAP plots [58]. The cell types were determined using a combination of marker genes identified from the literature and gene ontology. The marker genes were visualized by dot plot and t-SNE plots to reveal specific individual cell types.

## In vivo administration of sCtla-4-Ig

An *in vivo* sCtla-4-Ig administration assay was conducted to evaluate the potential therapeutic effect of sCTLA-4-Ig on intervention of a *ctla-4*-deficiency induced IBD-like phenotype. For this procedure, the *ctla-4*<sup>-/-</sup> zebrafish were i.p administered with recombinant soluble Ctla-4-Ig protein (sCtla-4-Ig, 2  $\mu$ g/g body weight) every other day until day 14. Fish that received an equal amount of human IgG isotype were used as control. The dose of sCtla-4-Ig was chosen based on its ability to significantly inhibit the mRNA expression of *il13* in Ctla-4-deficient zebrafish.

## Statistical analysis

Statistical analysis and graphical presentation were performed with GraphPad Prism 8.0. All data were presented as the mean  $\pm$  SD of each group. Statistical evaluation of differences was assessed using one-way ANOVA, followed by an unpaired two-tailed *t*-test. Statistical significance was

defined as  $*p < 0.05$ ,  $**p < 0.01$ ,  $***p < 0.001$ , and  $****p < 0.0001$ . All experiments were replicated at least three times.

## Data availability

All data generated or analyzed during this study are included in this article and its supplementary information files. The RNA-seq and scRNA-seq data for this study have been deposited in NCBI Gene Expression Omnibus (GEO) (<https://www.ncbi.nlm.nih.gov/geo/>) under accession numbers GSE255304 and GSE255303, respectively. The 16S rRNA sequencing data in this study have been deposited in the NCBI Sequence Read Archive (SRA) (<https://www.ncbi.nlm.nih.gov/sra/>) with an accession number of BioProject PRJNA1073727.

## Acknowledgements

We are grateful to Bio-ultrastructure analysis Lab of Analysis center of Agrobiology and environmental sciences, Zhejiang Univ in the TEM sample preparation and observation. We thank Hong Deng and Qiong Huang for advice and expertise in pathological analysis. We also thank She-long Zhang for two-photon laser confocal scanning microscope capture. This work was supported by grants from the National Natural Science Foundation of China (32173003), the National Key Research and Development Program of China (2018YFD0900503, 2018YFD0900505).

## Author Contributions

L. L. Q. and J. Z. S. conceived and designed the experiments. L. L. Q. and C. B. H. performed the experiments. L. L. Q., C. B. H., Q. Z., Y. W., A. F. L., L. X. X., Y. C., and J. Z. S. analyzed the data. L. X. X., D. D. F., and J. Z. S. contributed reagents/materials/analysis tools. L. L. Q., Y. C., L. X. X. and J. Z. S. wrote the manuscript. All authors reviewed the paper and provided comments.

## Conflict of Interest

The authors declare that they have no competing financial interests.

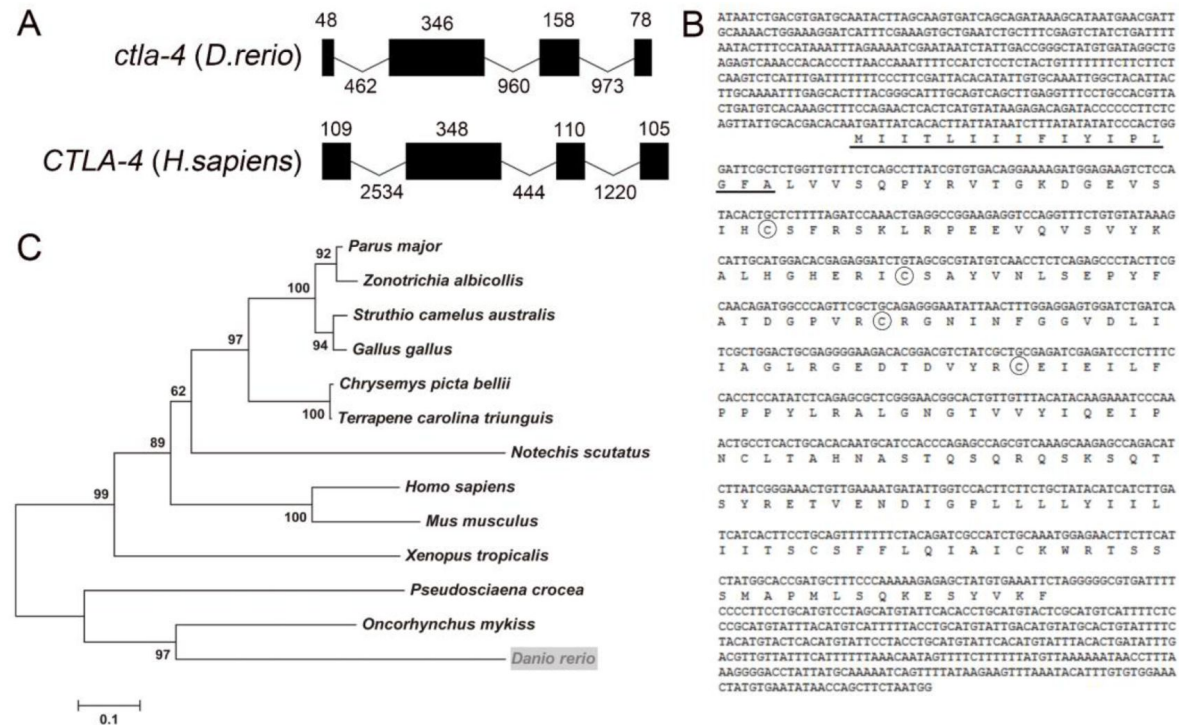
## Ethical approval and consent to participate

All animal experiments were performed with the approval of the Ethics Committee for Animal Experimentation of Zhejiang University.

## Supplemental Figures

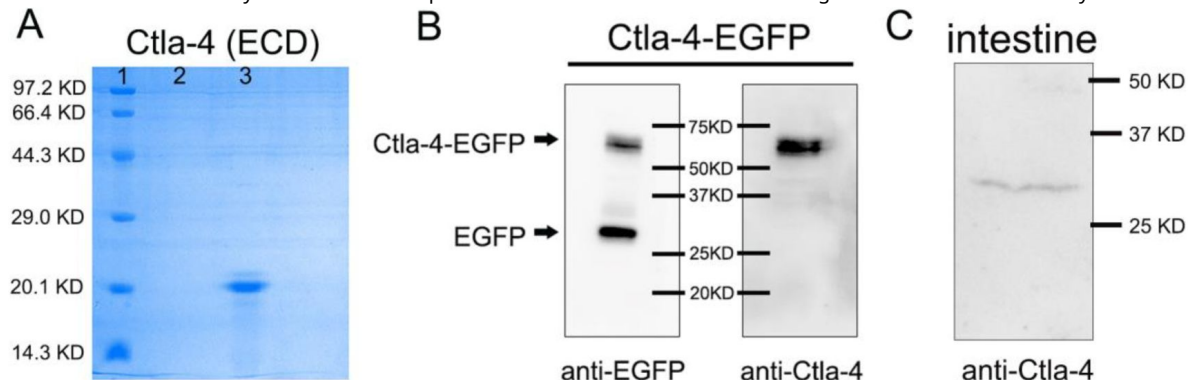
**Fig. S1**

The organization, sequence and phylogenetic analysis of zebrafish *ctla-4* gene. **A** Comparison of the intron/exon organizations of *ctla-4* gene in zebrafish and humans. Exons and introns are shown with black boxes and lines, and their size are indicated by the numbers found above and below the sequences respectively. **B** The nucleotide and amino acid sequences of *ctla-4* gene and Ctla-4 protein. The underline indicates the signal peptide, the circles represent the conserved cysteine residues. **C** Phylogenetic analysis of the relationship of Ctla-4 between zebrafish and other species. The unrooted phylogenetic tree was constructed through the neighbor-joining method based on the amino acid alignment (ClustalX) of amino acid sequences. The numbers represent the percentage bootstrap confidence derived from 500 replicates.



**Fig. S2**

Preparation of mouse anti-Ctla-4 antibody. **A** SDS-PAGE detection of the recombinant Ctla-4 protein with extracellular domain (ECD). Lane 1, 2 and 3 represent the protein markers, blank, and target protein, respectively. **B** Western blot analysis of the mouse anti-EGFP and anti-Ctla-4 antibodies that bind to the recombinant Ctla-4-EGFP fusion proteins expressed in HEK293T cells. **C** Western blot analysis of native Ctla-4 protein in zebrafish intestinal tissues using mouse anti-Ctla-4 antibody.



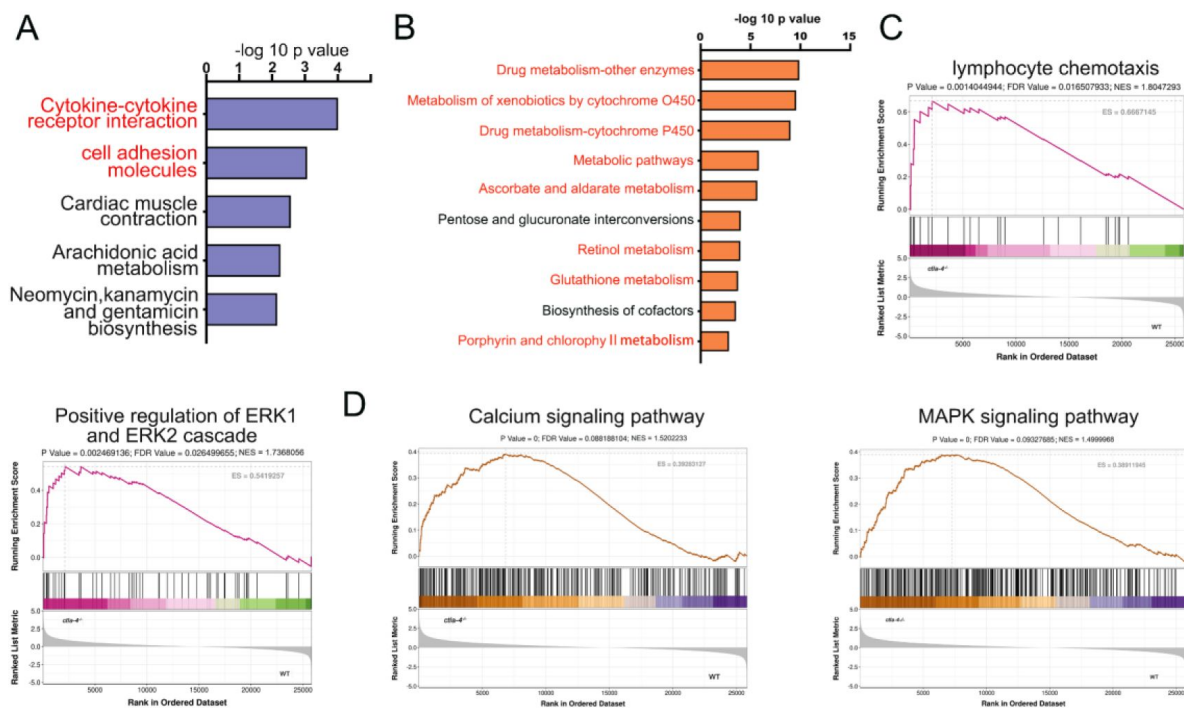


**Fig. S3**

Examination on the functional genes and pathways associated with the IBD-like phenotype in *ctla-4<sup>-/-</sup>* zebrafish. **A** Top 5 KEGG enrichment bar plot of up-regulated genes in *ctla-4<sup>-/-</sup>* zebrafish intestines versus wild-type zebrafish intestines. **B** Top 10 KEGG enrichment bar plot of down-regulated genes in *ctla-4<sup>-/-</sup>* zebrafish intestines versus wild-type zebrafish intestines. **C, D** Changes in the expression of genes associated with lymphocyte chemotaxis, positive regulation of ERK1/ERK2 cascades, Calcium and MAPK signaling pathways in the *ctla-4<sup>-/-</sup>* zebrafish intestines analyzed by using a collection of pre-defined gene sets retrieved from GO (**C**) and KEGG (**D**) database. The *p* value, false discovery rates (FDR) and normalized enrichment score (NES) are shown above each pathway graph.

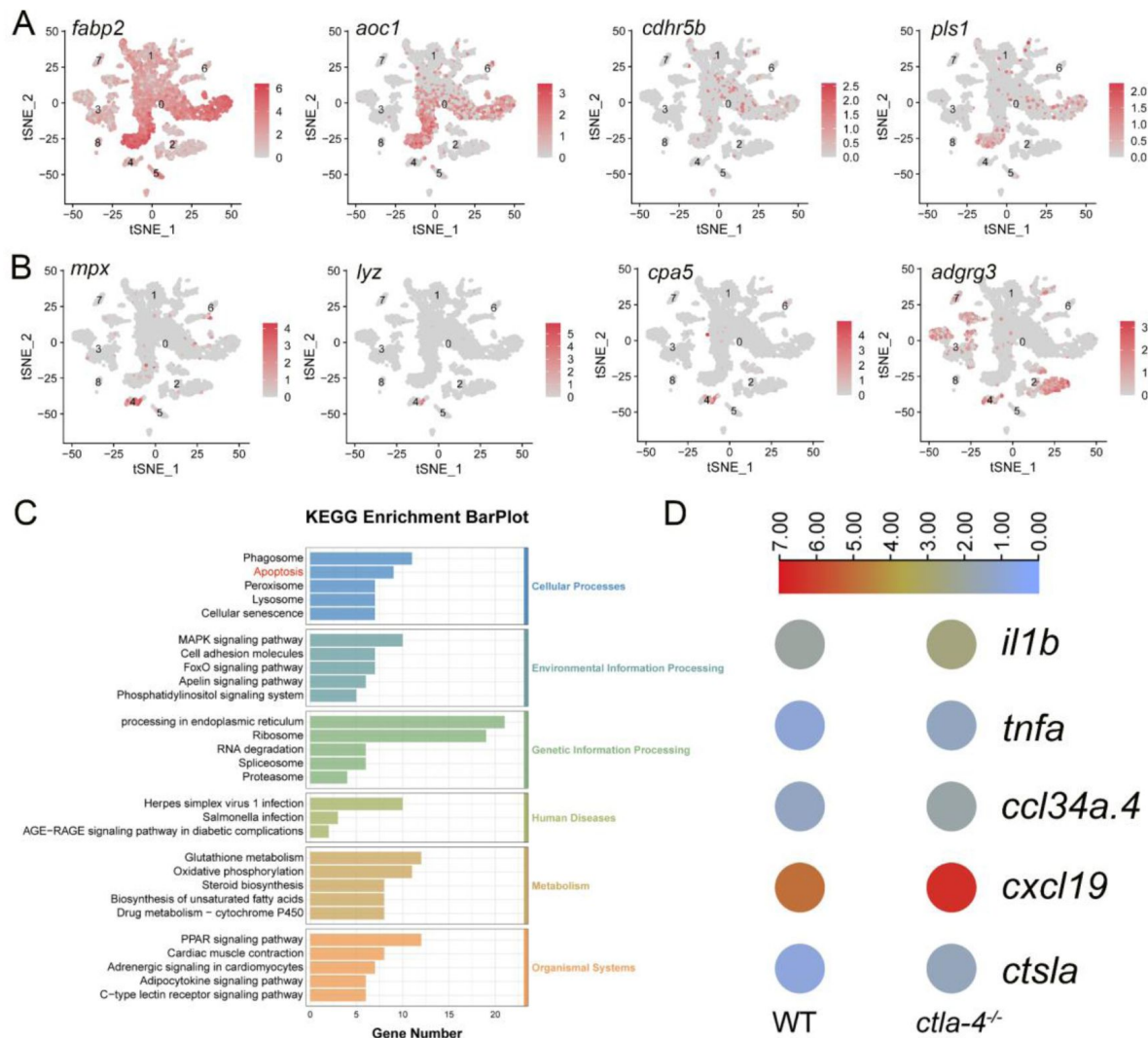


**Fig. S4**

Examination on the involvement of apoptotic process in epithelial cells and expression of inflammation-related genes in neutrophils and B cells in the intestines of *ctla-4<sup>-/-</sup>* zebrafish. **A** Expression map of the epithelial markers within the cell populations of the zebrafish intestines. **B** Expression map of the neutrophil markers within the cell populations of the zebrafish intestines. **C** KEGG enrichment bar plot of all DEGs from epithelial cells. **D** Heatmap of inflammation-related genes in B cells from wild-type and *ctla-4<sup>-/-</sup>* intestines.

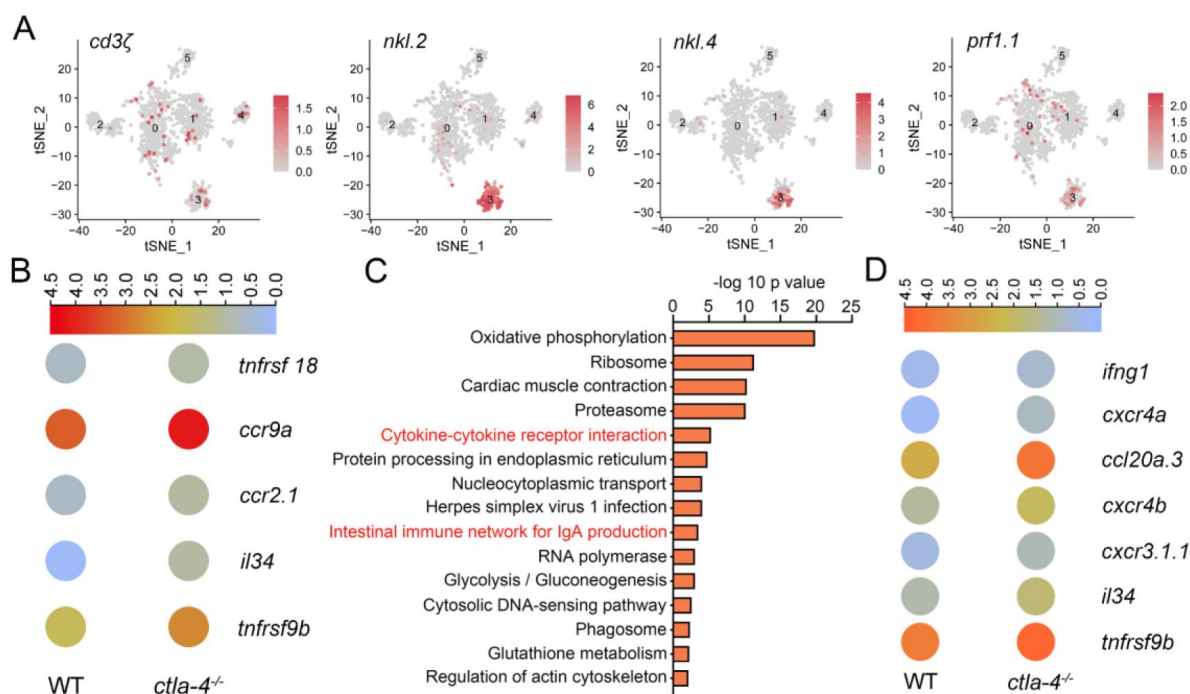


**Fig. S5**

Examination on the activation of T cell subsets in the intestines of *ctla-4<sup>-/-</sup>* zebrafish. **A** Marker gene expression in individual cluster identifying the cluster as NKT cells. **B** Heatmap of up-regulated genes involved in cytokine-cytokine receptor interaction in NKT cells among the wild-type and *ctla-4<sup>-/-</sup>* samples. **C** KEGG enrichment analysis showing top 15 terms of up-regulated genes in Cd8<sup>+</sup> T cells in *ctla-4<sup>-/-</sup>* samples versus wild-type samples. **D** Heatmap of up-regulated genes involved in cytokine-cytokine receptor interaction in Cd8<sup>+</sup> T cells among the wild-type and *ctla-4<sup>-/-</sup>* samples.

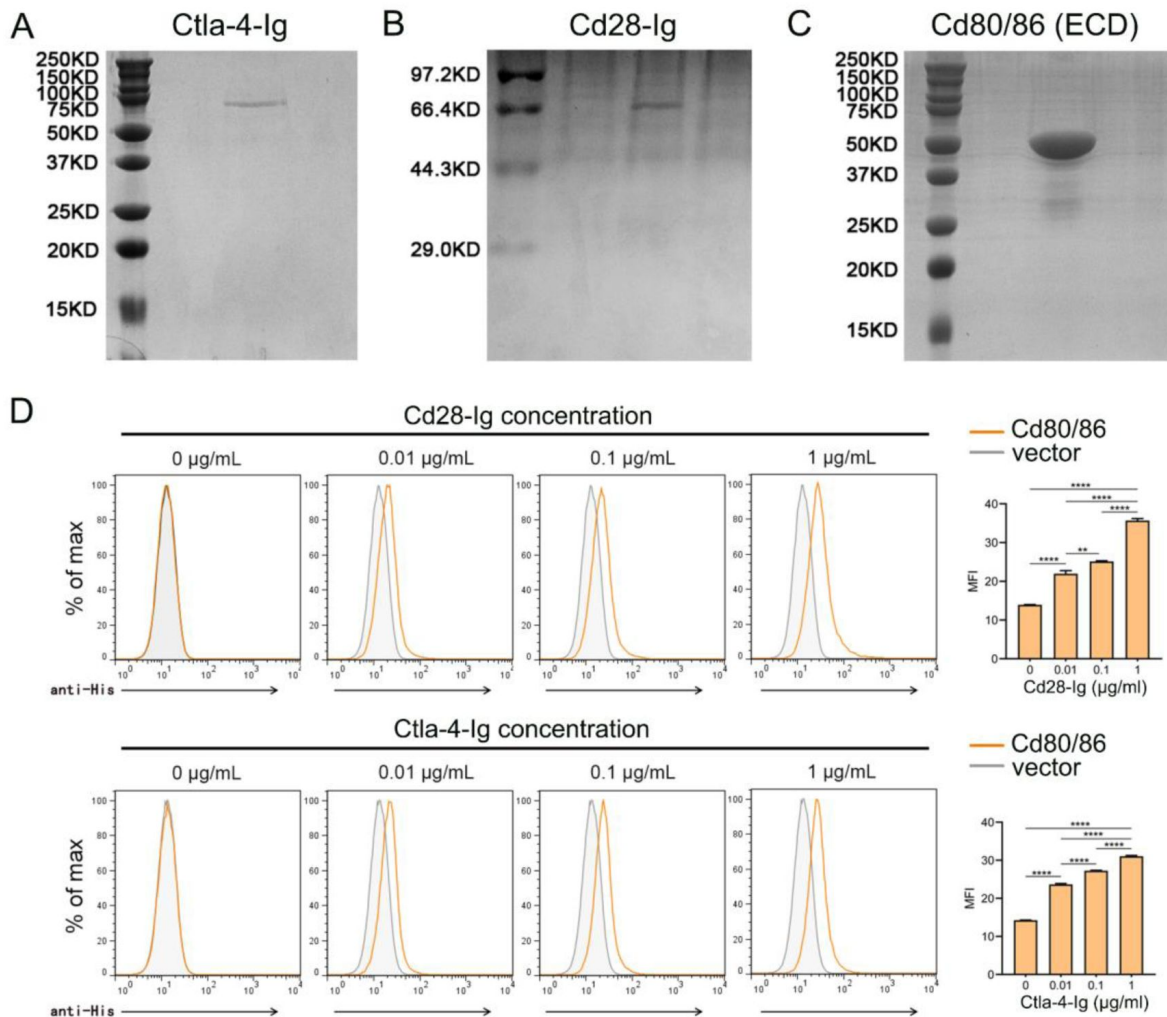


**Fig. S6**

Preparation of recombinant proteins and examination on the molecular interactions. **A-C** SDS-PAGE detection of the purified recombinant soluble Ctla-4-Ig (**A**) and Cd28-Ig (**B**) proteins and the Cd80/86 extracellular domain (ECD) (**C**) with Coomassie brilliant blue staining. **D** Flow cytometry analysis of the interaction between Cd80/86 and Cd28 (up), as well as Cd80/86 and Ctla-4 (down). Data are presented as mean  $\pm$  SD, which were calculated from three independent experiments. Statistical significance was evaluated using an unpaired Student's t test (\*\* $p < 0.01$ ; \*\*\* $p < 0.001$ ).

## References

1. Hodson R (2016) **Inflammatory bowel disease** *Nature* **540**:S97–S97 <https://doi.org/10.1038/540S97a>
2. Zhang Y Z, Li Y Y (2014) **Inflammatory bowel disease: Pathogenesis** *World J Gastroentero* **20**:91–99 <https://doi.org/10.3748/wjg.v20.i1.91>
3. Venema W T C U, Voskuil M D, Dijkstra G, Weersma R K, Festen E A M (2017) **The genetic background of inflammatory bowel disease: from correlation to causality** *J Pathol* **241**:146–158 <https://doi.org/10.1002/path.4817>
4. Loftus E V (2004) **Clinical epidemiology of inflammatory bowel disease: Incidence, prevalence, and environmental influences** *Gastroenterology* **126**:1504–1517 <https://doi.org/10.1053/j.gastro.2004.01.063>
5. Khor B, Gardet A, Xavier R J (2011) **Genetics and pathogenesis of inflammatory bowel disease** *Nature* **474**:307–317 <https://doi.org/10.1038/nature10209>
6. Neurath M F (2020) **Host-microbiota interactions in inflammatory bowel disease** *Nat Rev Gastro Hepat* **17**:76–77 <https://doi.org/10.1038/s41575-019-0248-1>
7. Kordjazy N, Haj-Mirzaian A, Haj-Mirzaian A, Rohani M M, Gelfand E W, Rezaei N, et al. (2018) **Role of toll-like receptors in inflammatory bowel disease** *Pharmacological Research* **129**:204–215 <https://doi.org/10.1016/j.phrs.2017.11.017>
8. Horowitz J E, Warner N, Staples J, Crowley E, Gosalia N, Murchie R, et al. (2021) **Mutation spectrum of NOD2 reveals recessive inheritance as a main driver of Early Onset Crohn's Disease** *Sci Rep-Uk* **11** <https://doi.org/10.1038/s41598-021-84938-8>
9. Duerr R H, Taylor K D, Brant S R, Rioux J D, Silverberg M S, Daly M J, et al. (2006) **A genome-wide association study identifies IL23R as an inflammatory bowel disease gene** *Science* **314**:1461–1463 <https://doi.org/10.1126/science.1135245>
10. Tremelling M, Berzuini C, Massey D, Bredin F, Price C, Dawson C, et al. (2008) **Contribution of TNFSF15 gene variants to Crohn's disease susceptibility confirmed in UK population** *Inflamm Bowel Dis* **14**:733–737 <https://doi.org/10.1002/ibd.20399>
11. Marengere L E, Waterhouse P, Duncan G S, Mittrucker H W, Feng G S, Mak T W (1996) **Regulation of T cell receptor signaling by tyrosine phosphatase SYP association with CTLA-4** *Science* **272**:1170–1173 <https://doi.org/10.1126/science.272.5265.1170>
12. Lee K M, Chuang E, Griffin M, Khattri R, Hong D K, Zhang W G, et al. (1998) **Molecular basis of T cell inactivation by CTLA-4** *Science* **282**:2263–2266 <https://doi.org/10.1126/science.282.5397.2263>
13. Yokosuka T, Kobayashi W, Takamatsu M, Sakata-Sogawa K, Zeng H, Hashimoto-Tane A, et al. (2010) **Spatiotemporal Basis of CTLA-4 Costimulatory Molecule-Mediated Negative Regulation of T Cell Activation** *Immunity* **33**:326–339 <https://doi.org/10.1016/j.immuni.2010.09.006>

14. Linsley P S, Greene J L, Brady W, Bajorath J, Ledbetter J A, Peach R (1994) **Human B7-1 (Cd80) and B7-2 (Cd86) Bind with Similar Avidities but Distinct Kinetics to Cd28 and Ctla-4 Receptors** *Immunity* **1**:793–801 [https://doi.org/10.1016/S1074-7613\(94\)80021-9](https://doi.org/10.1016/S1074-7613(94)80021-9)
15. Collins A V, Brodie D W, Gilbert R J, Iaboni A, Manso-Sancho R, Walse B, et al. (2002) **The interaction properties of costimulatory molecules revisited** *Immunity* **17**:201–210 [https://doi.org/10.1016/s1074-7613\(02\)00362-x](https://doi.org/10.1016/s1074-7613(02)00362-x)
16. Saito T, Yokosuka T, Hashimoto-Tane A (2010) **Dynamic regulation of T cell activation and co-stimulation through TCR-microclusters** *Febs Lett* **584**:4865–4871 <https://doi.org/10.1016/j.febslet.2010.11.036>
17. Repnik K, Potocnik U (2010) **CT60 Single-Nucleotide Polymorphism Is Associated with Slovenian Inflammatory Bowel Disease Patients and Regulates Expression of Isoforms** *DNA Cell Biol* **29**:603–610 <https://doi.org/10.1089/dna.2010.1021>
18. Xia B, Crusius J B A, Wu J, Zwiers A, van Bodegraven A A, Peña A S (2002) **CTLA-4 gene polymorphisms in Dutch and Chinese patients with inflammatory bowel disease** *Scand J Gastroentero* **37**:1296–1300 <https://doi.org/10.1080/003655202761020579>
19. Jiang T, Ge L Q, Chen Z T, Li C, Zhou F, Luo Y, et al. (2010) **Effect of cytotoxic T lymphocyte-associated molecule 4 1661 gene polymorphism on its expression and transcription in ulcerative colitis** *J Digest Dis* **11**:369–375 <https://doi.org/10.1111/j.1751-2980.2010.00462.x>
20. Bamias G, Delladetsima I, Perdiki M, Siakavellas S I, Goukos D, Papatheodoridis G V, et al. (2017) **Immunological Characteristics of Colitis Associated with Anti-CTLA-4 Antibody Therapy** *Cancer Invest* **35**:443–455 <https://doi.org/10.1080/07357907.2017.1324032>
21. Lo B C, Kryczek I, Yu J, Vatan L, Caruso R, Matsumoto M, et al. (2024) **Microbiota-dependent activation of CD4+ T cells induces CTLA-4 blockade-associated colitis via Fcγ receptors** *Science* **383**:62–70 <https://doi.org/10.1126/science.adh8342>
22. Erben U, Loddenkemper C, Doerfel K, Spieckermann S, Haller D, Heimesaat M M, et al. (2014) **A guide to histomorphological evaluation of intestinal inflammation in mouse models** *Int J Clin Exp Pathol* **7**:4557–4576
23. Heller F, Florian P, Bojarski C, Richter J, Christ M, Hillenbrand B, et al. (2005) **Interleukin-13 is the key effector Th2 cytokine in ulcerative colitis that affects epithelial tight junctions, apoptosis, and cell restitution** *Gastroenterology* **129**:550–564 <https://doi.org/10.1016/j.gastro.2005.05.002>
24. Butin-Israeli V, Bui T M, Wiesolek H L, Mascarenhas L, Lee J J, Mehl L C, et al. (2019) **Neutrophil-induced genomic instability impedes resolution of inflammation and wound healing** *J Clin Invest* **129**:712–726 <https://doi.org/10.1172/JCI122085>
25. Lees C W, Barrett J C, Parkes M, Satsangi J (2011) **New IBD genetics: common pathways with other diseases** *Gut* **60**:1739–1753 <https://doi.org/10.1136/gut.2009.199679>
26. Lee J C, Biasci D, Roberts R, Gearry R B, Mansfield J C, Ahmad T, et al. (2017) **Genome-wide association study identifies distinct genetic contributions to prognosis and susceptibility in Crohn's disease** *Nat Genet* **49**:262–268 <https://doi.org/10.1038/ng.3755>

27. Sinkala M, Nkhoma P, Mulder N, Martin D P (2021) **Integrated molecular characterisation of the MAPK pathways in human cancers reveals pharmacologically vulnerable mutations and gene dependencies** *Communications Biology* **4** <https://doi.org/10.1038/s42003-020-01552-6>
28. Trebak M, Kinet J P (2019) **Calcium signalling in T cells** *Nature Reviews Immunology* **19**:154–169 <https://doi.org/10.1038/s41577-018-0110-7>
29. Bernink J H, Peters C P, Munneke M, te Velde A A, Meijer S L, Weijer K, et al. (2013) **Human type 1 innate lymphoid cells accumulate in inflamed mucosal tissues** *Nat Immunol* **14**:221–229 <https://doi.org/10.1038/ni.2534>
30. Li J, Doty A L, Tang Y, Berrie D, Iqbal A, Tan S A, et al. (2017) **Enrichment of IL-17A(+) IFN-gamma(+) and IL-22(+) IFN-gamma(+) T cell subsets is associated with reduction of Nkp44(+) ILC3s in the terminal ileum of Crohn's disease patients** *Clin Exp Immunol* **190**:143–153 <https://doi.org/10.1111/cei.12996>
31. Martin J C, Chang C, Boschetti G, Ungaro R, Giri M, Grout J A, et al. (2019) **Single-Cell Analysis of Crohn's Disease Lesions Identifies a Pathogenic Cellular Module Associated with Resistance to Anti-TNF Therapy** *Cell* **178**:1493–1508 <https://doi.org/10.1016/j.cell.2019.08.008>
32. Buonocore S, Ahern P P, Uhlig H H, Ivanov I I, Littman D R, Maloy K J, et al. (2010) **Innate lymphoid cells drive interleukin-23-dependent innate intestinal pathology** *Nature* **464**:1371–1375 <https://doi.org/10.1038/nature08949>
33. Ermann J, Staton T, Glickman J N, de Waal Malefyt R, Glimcher L H (2014) **Nod/Ripk2 signaling in dendritic cells activates IL-17A-secreting innate lymphoid cells and drives colitis in T-bet<sup>-/-</sup>.Rag2<sup>-/-</sup> (TRUC) mice** *Proc Natl Acad Sci U S A* **111**:E2559–E2566 <https://doi.org/10.1073/pnas.1408540111>
34. Aparicio-Domingo P, Romera-Hernandez M, Karrich J J, Cornelissen F, Papazian N, Lindenberg-Kortleve D J, et al. (2015) **Type 3 innate lymphoid cells maintain intestinal epithelial stem cells after tissue damage** *J Exp Med* **212**:1783–1791 <https://doi.org/10.1084/jem.20150318>
35. Ott S J, Musfeldt M, Wenderoth D F, Hampe J, Brant O, Folsch U R, et al. (2004) **Reduction in diversity of the colonic mucosa associated bacterial microflora in patients with active inflammatory bowel disease** *Gut* **53**:685–693 <https://doi.org/10.1136/gut.2003.025403>
36. Manichanh C, Rigottier-Gois L, Bonnaud E, Gloux K, Pelletier E, Frangeul L, et al. (2006) **Reduced diversity of faecal microbiota in Crohn's disease revealed by a metagenomic approach** *Gut* **55**:205–211 <https://doi.org/10.1136/gut.2005.073817>
37. Zhao Q, Chang H, Zheng J, Li P, Ye L, Pan R, et al. (2023) **A novel Trmt5-deficient zebrafish model with spontaneous inflammatory bowel disease-like phenotype** *Signal Transduct Target Ther* **8** <https://doi.org/10.1038/s41392-023-01318-6>
38. Xu Z, Takizawa F, Casadei E, Shibasaki Y, Ding Y, Sauters T J C, et al. (2020) **Specialization of mucosal immunoglobulins in pathogen control and microbiota homeostasis occurred early in vertebrate evolution** *Sci Immunol* **5** <https://doi.org/10.1126/sciimmunol.aay3254>
39. Belzer C, de Vos W M (2012) **Microbes inside--from diversity to function: the case of Akkermansia** *ISME J* **6**:1449–1458 <https://doi.org/10.1038/ismej.2012.6>

40. Waterhouse P, Penninger J M, Timms E, Wakeham A, Shahinian A, Lee K P, et al. (1995) **Lymphoproliferative Disorders with Early Lethality in Mice Deficient in Ctla-4** *Science* **270**:985–988 <https://doi.org/10.1126/science.270.5238.985>
41. Tivol E A, Borriello F, Schweitzer A N, Lynch W P, Bluestone J A, Sharpe A H (1995) **Loss of Ctla-4 Leads to Massive Lymphoproliferation and Fatal Multiorgan Tissue Destruction, Revealing a Critical Negative Regulatory Role of Ctla-4** *Immunity* **3**:541–547 [https://doi.org/10.1016/1074-7613\(95\)90125-6](https://doi.org/10.1016/1074-7613(95)90125-6)
42. Hosseini A, Gharibi T, Marofi F, Babaloo Z, Baradaran B (2020) **CTLA-4: From mechanism to autoimmune therapy** *Int Immunopharmacol* **80** <https://doi.org/10.1016/j.intimp.2020.106221>
43. Sun W H, Zhang X M, Wu J, Zhao W D, Zhao S X, Li M L (2019) **Correlation of TSHR and CTLA-4 Single Nucleotide Polymorphisms with Graves Disease** *Int J Genomics* **2019** <https://doi.org/10.1155/2019/6982623>
44. Vergara A, De Felice M, Cesaro A, Gragnano F, Pariggiano I, Golia E, et al. (2023) **Immune-Checkpoint Inhibitor-Related Myocarditis: Where We Are and Where We Will Go** *Angiology* **12** <https://doi.org/10.1177/00033197231201929>
45. Kheiralla K E K (2021) **CTLA-4 (+49A/G) Polymorphism in Type 1 Diabetes Children of Sudanese Population** *Glob Med Genet* **8**:11–18 <https://doi.org/10.1055/s-0041-1723008>
46. Lin T W, Hu Y C, Yang Y H, Chien Y H, Lee N C, Yu H H, et al. (2022) **CTLA-4 gene mutation and multiple sclerosis: A case report and literature review** *J Microbiol Immunol* **55**:545–548 <https://doi.org/10.1016/j.jmii.2021.10.009>
47. Cutolo M, Sulli A, Paolino S, Pizzorni C (2016) **CTLA-4 blockade in the treatment of rheumatoid arthritis: an update** *Expert Rev Clin Immu* **12**:417–425 <https://doi.org/10.1586/1744666x.2016.1133295>
48. Chang M C, Chang Y T, Tien Y W, Liang P C, Jan I S, Wei S C, et al. (2007) **T-Cell regulatory gene CTLA-4 Polymorphism/Haplotype association with autoimmune pancreatitis** *Clin Chem* **53**:1700–1705 <https://doi.org/10.1373/clinchem.2007.085951>
49. Fathima N, Narne P, Ishaq M (2019) **Association and gene-gene interaction analyses for polymorphic variants in CTLA-4 and FOXP3 genes: role in susceptibility to autoimmune thyroid disease** *Endocrine* **64**:591–604 <https://doi.org/10.1007/s12020-019-01859-3>
50. Zeissig S, Petersen B S, Tomczak M, Melum E, Huc-Claustre E, Dougan S K, et al. (2015) **Early-onset Crohn's disease and autoimmunity associated with a variant in CTLA-4** *Gut* **64**:1889–1897 <https://doi.org/10.1136/gutjnl-2014-308541>
51. Angelino G, Cifaldi C, Zangari P, Di Cesare S, Di Matteo G, Chiriaco M, et al. (2021) **Gastric cancer, inflammatory bowel disease and polyautoimmunity in a 17-year-old boy: CTLA-4 deficiency successfully treated with Abatacept** *Eur J Gastroen Hepat* **33**:E1051–E1056 <https://doi.org/10.1097/Meg.0000000000002185>
52. Liu J Z, van Sommeren S, Huang H L, Ng S C, Alberts R, Takahashi A, et al. (2015) **Association analyses identify 38 susceptibility loci for inflammatory bowel disease and highlight shared genetic risk across populations** *Nat Genet* **47** <https://doi.org/10.1038/ng.3359>

53. Al-Sadi R, Guo S H, Ye D M, Dokladny K, Alhmoud T, Ereifej L, et al. (2013) **Mechanism of IL-1b Modulation of Intestinal Epithelial Barrier Involves p38 Kinase and Activating Transcription Factor-2 Activation** *Journal of Immunology* **190**:6596–6606 <https://doi.org/10.4049/jimmunol.1201876>
54. Al-Sadi R, Guo S H, Ye D M, Ma T Y (2013) **TNF- $\alpha$  Modulation of Intestinal Epithelial Tight Junction Barrier Is Regulated by ERK1/2 Activation of Elk-1** *Am J Pathol* **183**:1871–1884 <https://doi.org/10.1016/j.ajpath.2013.09.001>
55. Zhu L Y, Lin A F, Shao T, Nie L, Dong W R, Xiang L X, et al. (2014) **B Cells in Teleost Fish Act as Pivotal Initiating APCs in Priming Adaptive Immunity: An Evolutionary Perspective on the Origin of the B-1 Cell Subset and B7 Molecules** *Journal of Immunology* **192**:2699–2714 <https://doi.org/10.4049/jimmunol.1301312>
56. Kohl M, Wiese S, Warscheid B (2011) **Cytoscape: software for visualization and analysis of biological networks** *Methods Mol Biol* **696**:291–303 [https://doi.org/10.1007/978-1-60761-987-1\\_18](https://doi.org/10.1007/978-1-60761-987-1_18)
57. McGinnis C S, Murrow L M, Gartner Z J (2019) **DoubletFinder: Doublet Detection in Single-Cell RNA Sequencing Data Using Artificial Nearest Neighbors** *Cell Syst* **8** <https://doi.org/10.1016/j.cels.2019.03.003>
58. Cronan M R, Hughes E J, Brewer W J, Viswanathan G, Hunt E G, Singh B, et al. (2021) **A non-canonical type 2 immune response coordinates tuberculous granuloma formation and epithelialization** *Cell* **184**:1757–1774 <https://doi.org/10.1016/j.cell.2021.02.046>
59. Hu C B, Wang J, Hong Y, Li H, Fan D D, Lin A F, et al. (2023) **Single-cell transcriptome profiling reveals diverse immune cell populations and their responses to viral infection in the spleen of zebrafish** *Faseb J* **37** <https://doi.org/10.1096/fj.202201505RRRR>

## Editors

Reviewing Editor

**B  r  nice Benayoun**

University of Southern California, Los Angeles, United States of America

Senior Editor

**Tadatsugu Taniguchi**

University of Tokyo, Tokyo, Japan

## Reviewer #1 (Public review):

"Unraveling the Role of Ctla-4 in Intestinal Immune Homeostasis: Insights from a novel Zebrafish Model of Inflammatory Bowel Disease" suggests the identification of the zebrafish homolog of ctla-4 and generates a 14bp deletion/early stop codon mutation that is viable. This mutant exhibits an IBD-like phenotype, including decreased intestinal length, abnormal intestinal folds, decreased goblet cells, abnormal cell junctions between epithelial cells, increased inflammation, and alterations in microbial diversity. Bulk and single-cell RNA-seq show upregulation of immune and inflammatory response genes in this mutant (especially in neutrophils, B cells, and macrophages) and downregulation of genes involved in adhesion and tight junctions in mutant enterocytes. The work suggests that the makeup of immune cells within the intestine is altered in these mutants, potentially due to changes in lymphocyte

proliferation. Introduction of recombinant soluble Ctla-4-Ig to mutant zebrafish rescued body weight, histological phenotypes, and gene expression of several pro-inflammatory genes, suggesting a potential future therapeutic route.

**Strengths:**

- Generation of a useful new mutant.
- The demonstration of an IBD-like phenotype in this mutant is extremely comprehensive.
- Demonstrated gene expression differences provide mechanistic insight into how this mutation leads to IBD-like symptoms.
- Demonstration of rescue with a soluble protein suggests exciting future therapeutic potential.
- The manuscript is mostly well organized and well written.

**Weaknesses:**

- Given the sequence similarity between CTLA-4 and its related receptor CD28, and the difference in subcellular localization of this protein vs. human CTLA-4, some confusion remains about which gene is mutated in this manuscript (CD28 or CTLA-4/CD152).
- Some conclusions made from scRNAseq data (e.g. increased apoptosis, changes in immune cell numbers) could potentially result from dissociation artifacts and would be stronger with validation staining.
- The Methods section is woefully incomplete and describes fewer than half of the experiments performed in this manuscript.

<https://doi.org/10.7554/eLife.101932.1.sa2>

**Reviewer #2 (Public review):**

**Summary:**

The authors aimed to elucidate the role of Ctla-4 in maintaining intestinal immune homeostasis by using a novel Ctla-4-deficient zebrafish model. This study addresses the challenge of linking CTLA-4 to inflammatory bowel disease (IBD) due to the early lethality of CTLA-4 knockout mice. Four lines of evidence were shown to show that Ctla-4-deficient zebrafish exhibited hallmarks of IBD in mammals:

- (1) impaired epithelial integrity and infiltration of inflammatory cells;
- (2) enrichment of inflammation-related pathways and the imbalance between pro- and anti-inflammatory cytokines;
- (3) abnormal composition of immune cell populations; and
- (4) reduced diversity and altered microbiota composition. By employing various molecular and cellular analyses, the authors established ctla-4-deficient zebrafish as a convincing model of human IBD.

**Strengths:**

The characterization of the mutant phenotype is very thorough, from anatomical to histological and molecular levels. The finding effectively established ctla-4 mutants as a novel zebrafish model for investigating human IBD. Evidence from the histopathological and transcriptome analysis was very strong and supported a severe interruption of immune system homeostasis in the zebrafish intestine. Additional characterization using sCtla-4-Ig

further probed the molecular mechanism of the inflammatory response and provided a potential treatment plan for targeting Ctla-4 in IBD models.

**Weaknesses:**

Since CTLA-4 is one of the most well-established immune checkpoint molecules, it is not clear whether the ctla-4 mutant zebrafish exhibits inflammatory phenotypes in other tissues than the intestine. Although the evidence for intestinal phenotypes is clear and similar to human IBD, it can be ambiguous whether the mutant is a specific model for IBD, or abnormal immune response in general.

To probe the molecular mechanism of Ctla-4, the authors used a spectrum of antibodies that target Ctla-4 or its receptors. The phenotype assayed was lymphocyte proliferation, while it was the composition rather than the number of immune cell number that was observed to be different in the scRNASeq assay. Although sCtla-4 has an effect of alleviating the IBD-like phenotypes, I found this explanation a bit oversimplified.

<https://doi.org/10.7554/eLife.101932.1.sa1>

**Reviewer #3 (Public review):**

**Summary:**

The current study on the mutant zebrafish for IBD modeling is worth trying. The author provided lots of evidence, including histopathological observation, gut microflora, as well as intestinal tissue or mucosa cells' transcriptomic data. The multi-omic study has demonstrated the enteritis pathology at multi levels in zebrafish model. However, poor writing of methods and insufficient discussion of current findings were the main defects.

**Strengths:**

The important immune checkpoint of Treg cells was knocked out in zebrafish, and the enteritis was found then. It could be a substitution of the mouse knockout model to investigate the molecular mechanism of gut disease.

**Weaknesses:**

- (1) The use of the English language requires further editing.
- (2) The background of this study has not been introduced sufficiently.
- (3) The medical concepts were overstated for immune cell populations.
- (4) A lot of methods were not provided.
- (5) The age of fish varied a lot in this study.
- (6) The pathological index can't reflect the detailed changes in intestinal mucosa.
- (7) A lot of findings reflected by the current were not discussed.
- (8) The structuring of the text is poor and lacks good logic.

<https://doi.org/10.7554/eLife.101932.1.sa0>